Leucine-rich repeats and immunoglobulin-like domain protein 1 in murine model of wound healing and p27 protein modeling

By

Amania Anwar

(NUST201260351MASAB91012F)

Atta-Ur-Rahman School of Applied Biosciences

National University of Science & Technology

Islamabad, Pakistan

2014

Leucine-rich repeats and immunoglobulin-like domain protein 1 in murine model of wound healing and p27 protein modeling

By

Amania Anwar

(NUST201260351MASAB91012F)

A thesis submitted in partial fulfillment of the requirement for the degree of masters of Philosophy

In

Health Care Biotechnology

Atta-Ur-Rahman School of Applied Biosciences

National University of Science & Technology

Islamabad, Pakistan

2014

Dedicated to

my loving Parents,

siblings Farooq, Waqas and Basum

for their endless love, encouragement and support

Acknowledgments

All praises to **Allah** Almighty, the Creator of the universe and the origin of all knowledge and wisdom to mankind. Nothing can sustain, without His will. Who empowered me to successfully complete my research work. All regards to the **Holy Prophet Hazrat Muhammad (SA**W) whose teachings are a source of guidance for me.

It is an honour to express my deep gratitude to **Dr. Peter John**, Professor and Director General, of Atta-Ur- Rehman School of Applied Biosciences for providing me an opportunity to conduct research in a friendly environment. I feel great pleasure to take this opportunity to express my regards and appreciation to my respected, profound and learned supervisor, **Dr. Sheeba Murad Mall** for her kind supervision and guidance. I would also owe my gratitude to my external examiner **Dr. Aneesa Sultan for** and internal thesis committee members **Dr. Sobia Manzoor** and **Dr. Alvina Gul** for their support. My acknowledgments would not be complete without paying my regard to **Dr. Amjad Ali** and **Sir Rehan**. They helped me in bioinformatics. Most importantly I would like to acknowledge **Dr. Arshad Mumtaz** of National Institute of Health and his team for guiding me in sample preparation. Further I would like to thank my research fellows: Faryal, Noreen, Orooj, Sanila, Sherbano, Atooba, Azkia and Tayyaba.

TABLE OF CONTENTS

LIST OF ACRONYMS

%	Percentage
~	Approximately
°C	Degree Celsius
AKT1	RAC-alpha serine/threonine-protein kinase
Bp	Base Pair
CDKN1B	Cyclin dependent kinase inhibitor
CRM1	Chromosome maintenance region 1
EGFR	Epidermal growth factor receptor
IFE	Interfollicular epidermis
IHC	Immunohostochemistry
JNK	c-Jun N-terminal kinases
LRIG	Leucine-rich repeats and immunoglobulin-like domain protein
MAPK	Mitogen activated protein kinase
MgCl2	Magnesium Chloride
PLC gamma	Phospholipase gamma
PI-3 K	Phosphoinositide 3-kinase

Ml	Milli Liter
mM	Milli Molar
mRNA	Messenger Ribonucleic Acid
MU	Million Units
Ng	Nanogram
NCBI	National Center for Biotechnology Information
S	Serine
TGF α	Tumor Growth factor α
T	Threonine
UV	Ultraviolet
V	Valine
VEGF	Vascular endothelial growth factor
WHO	World Health organization

LIST OF TABLES

LIST OF FIGURES

ABSTRACT

Leucine-rich repeats and immunoglobulin-like domains protein 1 (LRIG1) was first isolated by Nilsson in 2001 and since then its role as a tumor suppressor has been widely studied. In epithelial cancers, LRIG1 is known to suppress epidermal growth factor receptor's (EGFR) downstream signaling. Moreover, mice deficient in LRIG-1 gene show histopathological features similar to psoriatic skin lesions. Therefore, we aimed to explore the LRIG-1 expression in full thickness epidermal excisional wound healing murine model. Female balb/c mice skin tissue sections were taken at day 1, 2, 3, 6 and day 14 after wounding. The highest expression of LRIG-1 was found to be expressed at day 0. There was a gradual decline in the LRIG-1 expression during the most of the wound healing stages. The regain of LRIG1 expression on day 14 marks the importance of LRIG1 in normal non-proliferative skin status or homeostasis. In addition to this, we used abinitio tools to model p27 protein also reported as a tumor suppressor protein often found to be down regulated in the EGFR over expressing epithelial cells. Novel mutations: c.4_6insGTT and c.520delA in p27 gene were reported by a previous colleague from our lab. These mutations can affect the post-translational modifications of the p27 proteins. Therefore, we were interested to explore the functional implications of these mutations. It was found that the novel mutation in p27 protein affects its interaction with AKT, furthermore, it was found that p27 nuclear localization was most likely to occur. Thus, this prediction model outlines few of the ways how p27 mutations may alter its function thus playing a possible pathogenic role in cancer progression.

Chapter 1

INTRODUCTION

Wounds are induced due to disruption of the skin's integrity via injury or disease which requires well orchestrated complex molecular events for optimal healing. However, de-synchronized biological pathways sometimes results in limb amputations and mortality. In United States alone each year 1.25 million people suffer from burns (Brigham and Mcloughlin, 1996) and 6.5 million have chronic skin ulcers due to pressure, venous stasis, or diabetes mellitus (Irvine and Calif, 1997). Non healing wounds are a serious health care dilemma globally, despite the availability of treatment. Further, wound management is expensive for instance the approximate cost of every episode of leg ulcers is €6650 and foot ulcers is €10000 which is assumed to rise with increasing elderly and diabetic patients (Gottrup *et al.*, 2010). Although the several phases of wound healing are known but there are many aspects that need to be addressed especially the mechanisms underlying abnormal wound healing as in chronic ulcers, burns and hypertrophic scars (Stadelmann *et al.*, 1998) (Hunt *et al.*, 1999).

Wound healing is a dynamic process divided in three phases: inflammation, tissue formation and remodeling which integrate various mediators. Cutaneous injury leads to disruption of blood vessels and leakage of blood constituents. The blood clot rich in fibrinogen and platelets, re-establishes hemeostasis and extracellular matrix for cell migration (Singer and Clark, 1999). An acute inflammatory phase is initiated within

hour after wounding, numerous vasoactive mediators and chemotactic factors are generated which recruit inflammatory leukocytes (Clark, 1996). Infiltrating neutrophils clean the wounds from foreign particles and bacteria. Further, macrophages secrete growth factors such as platelet-derived growth factor and vascular endothelial growth factor, which stimulate fibroblast to proliferate and migrate to the site of the wound (Heldin *at al.*, 1996).

A granulation tissue also known as stroma begins to form after four days post injury. New capillaries confer stroma with granular appearance, carry oxygen and nutrients to sustain cell metabolism (Hunt, 1980) Macrophages provide growth factors which are essential for mediating angiogenesis and fibroplasias (Singer and Clark, 1999). Moreover, fibroblasts regulate the synthesis, deposition and remodeling of the extracellular matrix. It provides a scaffold and conduit for cell migration, thus act as a limiting factor in the formation of granulation tissue (Greiling and Clark, 1997). During the re-epithelization, epidermal cells actively proliferate, break hemidesmosomal links between the epidermis and the basement membrane and migrate laterally to the site of the wound margin (Clark, 1990; Larjava *et al.*, 1993; Clark *et al.*, 1996). Keratinocytes migration continues till the wound edges merge at wound junction (Stadelmann *et al*, 1998). The remodeling phase lasts up to a year, involves simultaneous synthesis and catabolism of collagen by fibroblast and metalloproteinases respectively (Stadelmann *et al.*, 1998; Singer and Clark, 1999).

In the past decade, scientists have partially elucidated the role of various exogenous and endogenous cytokines and growth factors in wound healing. Epidermal growth

factor receptor (EGFR) is an important receptor which responds to several growth factors and activates major signaling pathways activated including PI3 kinase, Ras-Raf (MAPK), JNK and PLC gamma. These signaling systems are particularly important for cell proliferation adhesion and motility, as a protection against apoptosis at the cellular level, and to promote invasion and angiogenesis at the physiological level in normal cells (Suzanne *et al.*, 2011).

In addition, studies have shown that epidermal growth factor receptor (EGFR) and its ligands are involved in the migration and proliferation of keratinocytes adjacent to wound margins (Werner and Grose, 2003). Stoscheck et al used enzyme-linked immunosorbent assay and histological methods to detect EGFR levels. The expression of EGFR and its ligand were found to correlate with the epidermal thickness thus this expression pattern suggested that EGFR has an implication in re-epithelialization (Stoscheck *et al.*, 1992). In human burn wounds, EGFR was found to express in wound epidermis, hair follicles, sweat ducts and sebaceous glands (Wenczak *et al.*, 1992). Moreover, EGF and EGF receptors showed decreased expression in incisional wounds of aged mice in comparison with young mice (Ashcroft *et al.*, 1997). Further, this notion was confirmed when exogenously expressed EGFR accelerated wound re-epithelization in porcine partial-thickness incisional wound model (Nanney *et al*, 2000). Moreover, in the presence of EGFR, the transcriptional expression of several growth factors involved in wound healing was repressed (Stoll *et al*, 1997). A recent study compared the cellular events of wound healing in EGFR null mice and EGFR wild type mice. It was found that EGFR

regulates keratinocyte proliferation, re-epitheliazation, inflammation and angiogenesis (Susan *et al*., 2004).

Besides wound healing process, epidermal growth factor receptors (EGFRs) have been extensively studied in context with human cancers and have demonstrated to promote hall marks of cancers. Additionally, EGFRs have been found mutated and over expressed in various epithelial cancers including breast, ovarian, lung, bladder, head and neck cancers (Salomon *et al* .,1995).

Activated EGFRs regulate the de novo expression of EGFR inhibitors. Recently, Leucine-rich repeats and immunoglobulin-like domains protein 1 (LRIG1) was found as a potent inducible feedback inhibitors of EGFRs (Gur *et al*., 2004). LRIG1 gene is located on human chromosome 13p14 and expressed ubiquitously in tissues. It encodes a transmembrane cell-surface protein with extracellular leucine-rich repeats and immunoglobulin-like domains, followed by a cytoplasmic tail. LRIG1 interacts with EGFR and degrades it in Cbl dependent and independent manner. (Gur *et al*., 2004: Stutz *et al*, 2008). Where, deletion of Lrig1 leads to increased levels of ErbB receptors in intestine and enhanced EGFR signaling in keratinocytes (Suzuki *et al*, 2002; Powell *et al*, 2012). Screening of Lrig1 locus for mutations showed deletions in nasopharyngeal (Sheu *et al*, 2009), renal (Willers *et al*, 1996), colorectal, glioblastoma and breast cancers (Maitra *et al*, 2001)

Moreover, LRIG-1 protein was expressed in epidermal basal cells and hair follicle cells of the normal mouse-tail skin. In addition, mice deficient in LRIG-1 gene showed histopahological features similar to psoriatic epidermis: the epidermis became

thick with increased proliferation and altered differentiation of keratinocytes (Suzuki *et al*., 2002). More recently, a study has found that Lrig1 is expressed by the intestinal stem cells and it controls homeostasis within the stem-cell compartment by regulating EGFR family of receptor's signaling which are highly expressed by stem cell niche (Wong *et al*., 2012). These findings have conferred Lrig1 as an important tumor suppressor and it regulates the proliferation of epithelial cells.

Wound healing and tumorigenesis are complex processes that depend on parallel molecular mechanisms (Arwert *et al*., 2012). The stem cells adapt a new location and contribute towards wound healing and tumor formation. A key difference is that wound healing is a self-limiting process. On the contrary, tumor formation is characterized by uninterrupted activation of pathways involved (Arwert *et al*., 2012). Additionally, in epithelial cells over expression of EGFR family members initiate p27 proteolysis and in the presence of EGFR inhibitors the p27 proteolysis is reversed. Thus, by identifying pathways involved in EGFR driven p27 proteolysis it may predict new therapeutic agent against EGFR in cancers (Chu *et al*., 2008).

P27 kip1 is a potent regulator, which in response to anti proliferative signals inhibit cells to progress from G1 to S phase of cell cycle by binding and inactivating cyclin E or A CDK2 complexes (Lee *et al*., 1995; Toyoshima, 1994; Polyak *et al*., 1994). However, p27 kip1 promotes cell cycle progression by its redistribution between different cyclins-CDK complexes (Toyoshima and Hunter, 1994). In addition, the activity of p27 is regulated within the cellular compartments via ubiquitin-mediated proteasomal degradation and subcellular localization (Sherr and

Roberts, 1999) (Borriello *et al.*, 2007). Thus, the levels of p27 need to be strictly maintain in the cellular compartments and any abnormal change can lead to cancer development. In order to exert its inhibitory activity p27kip1 must be located in the nucleus. P27 kip1 contains a nuclear localization signal at its Carboxyl terminus which mediates its nuclear export followed by interaction with c-Jun activation domain-binding protein-1 (Jab1) or chromosome region maintenance 1 (CRM1) via alpha serine/threonine protein kinase-1 (AKT1) phosphorylated p27 at S10 (Tomoda *et al.*, 1999; Ishida *et al.*, 2002; Boehm *et al.*, 2002). Additionally, AKT1 phophorylates p27 at T157 and T198 and phosphorylation at these sites promote binding of p27 with 14-3-3 instead of nuclear shuttling proteins, which impairs nuclear import.

We hypothesize as a negative regulator of EGFR1 and a stem cell marker, there may be a differential expression of LRIG1 at different stages of wound healing. Thus the aim of the present study is to determine the protein expression of LRIG1 in full thickness excisional wounds in murine model of wound healing. In addition this study also aims to model p27 protein and to predict the implication of a frameshift mutation in p27 in its interaction with alpha serine/ threonine protein kinase-1 (AKT1).

Chapter 2

REVIEW OF LITERATURE

2.1LEUCINE- RICH REPEATS AND IMMUNOGLOBULIN-LIKE DOMAIN PROTEIN (LRIG) FAMILY

2.1.1 Structural features of LRIG family

The human LRIG gene family comprises of three paralogous genes namely LRIG1 and LRIG2 and LRIG3. The LRIG genes encode integral cell surface proteins, which consist of an extracellular region having leucine rich repeats flanked by cysteines residues at N and C terminal, followed by three immunoglobulin domains, a transmembrane domain and cytoplasmic tail (Hedman and Henriksson, 2007). The ectodomain, transmembrane region and the proximal domain of the cytoplasmic domain contains aminoacid which are highly conserved in all LRIGs, implying they might have a similar function (figure 2.1) (Guo *et al.*, 2004). *Mus musculus* express LRIG1, LRIG2 and LRIG3 which share 80%, 87% and 86% amino acid sequence identity with respective human Lrig orthologs (shown in figure 2.2). In addition *Caenorhabditis elegans* and the *Ciona intestinalis* both contain one Lrig ortholog (Gumienny, 2010). Moreover, *pufferfish* and *Fugu* share more than 60% amino acid sequence similarity with human orthologs thereby establishing the fact that LRIG proteins have remained conserved during evolution (Guo *et al.*, 2004).

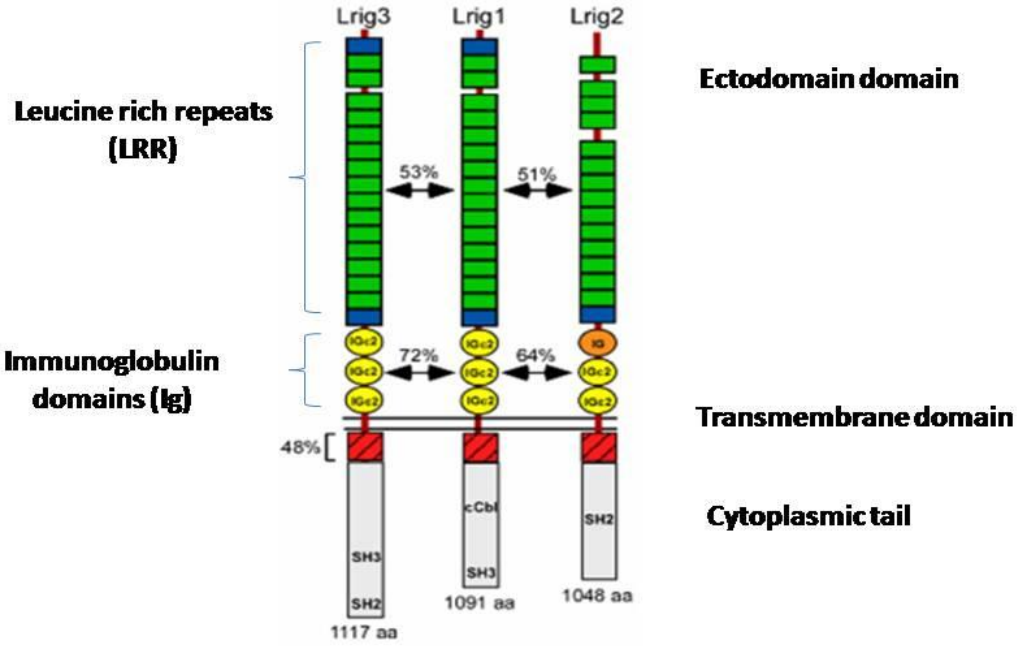

Figure 2.1: Structural representation of LRIG family members. LRIG1 and LRIG3 share same number of leucine rich repeats (LRR) and immunoglobulin domains with 53% and 72% homology respectively. On the contrary, LRIG2 is deprived of an N terminal LRR and has a different immunoglobulin domain. In intracellular domain all three share identical stretch of 48 aminoacids. However, the cytoplasmic tail consisted of either SH3 or SH2 domain varies in length for all three. LRIG1 is the only member which contains c-CbL binding domain adapted from Abraira *et al*., 2010

	Human LRIG1	Human LRIG2	Human LRIG3
Human LRIG1	100.0	41.3	46.8
Human LRIG2		100.0	54.0
Human LRIG3			100.0
Mouse Lrig1	80.1		
Mouse Lrig2		87.1	
Mouse Lrig3			85.5
Fugu 72788	69.0		
Fugu 81160		64.6	
Fugu 77189			75.1
Ciona	31.3	33.1	34.4

[a] For mouse and *Fugu* LRIGs, only comparisons to human orthologs are shown.

Figure 2.2: Percentage of aminoacid identity between LRIG1-LRIG3 orthologs adapted from (Guo *et al.*, 2004).

2.1.2 Genomic localization of the Human and Mouse LRIG genes

Mouse LRIG1 is found at chromosomes 6D2 and LRIG2 at 3F2+2. Moreover, mouse LRIG3 is located at chromosome 10D2 (Guo *et al.*, 2004). The human LRIG1, LRIG2 and LRIG3 were found to be located at 3p14, 1p13 and 12q13.2 respectively. These loci are located at syntenic regions corresponding to mouse loci (Nilsson, 2001).

2.1.3 LRIG expressions in tissues

LRIG proteins are ubiquitously expressed in mouse tissues which depict that LRIGs have functions which are essential for most of the cell types and organs. However, all LRIGs show different intensity of expressions in same tissues (Hedman

et al., 2002). LRIG1 and LRIG3 are highly expressed in ovary and embryo. Moreover, LRIG2 is expressed in testicles. In addition, Human LRIG paralogs in comparison with mouse paralogs show different expression levels. LRIG1 is expressed in liver, brain, stomach, small intestine, and skeletal muscle. LRIG2 shows high transcriptional levels in uterus, ovary, and skin and LRIG3 in stomach, thyroid, and skin (Guo *et al.*, 2004).

2.2 LRIGS IN HUMAN CANCERS

2.2.1 LRIG as prognostic markers

Several recent studies have focused on the lrig1 expression and its prognostic value in different cancers**.** Thomasson et al. studied expressions of LRIG1 and EGFR in renal cell carcinomas. They observed increased EGFR/LRIG1 ratio in conventional renal cell carcinoma suggesting LRIG1 acts as tumour suppressor by counteracting tumour-promoting properties of EGFR (Thomasson *et al*, 2003). Moreover, Tanemura et al showed LRIG1 was highly expressed in well-differentiated lesions of cutaneous SCC and it has the potential of an excellent prognostic indicator for cutaneous SCC. Further, Lrig1 expressions inversely correlated with metastatic rate and directly with patients survival rate (Tanemura *et al.*, 2005). Another study associated high LRIG1 expression with better survival in early stages of uterine cervical carcinoma (Lindstrom *et al.*, 2008). On the contrary, LRIG2 showed an independent prognostic potential with poor patient survival in oligodentroglial tumors (Holmlund *et al.*, 2009). In addition high LRIG2 expression with low LRIG1 expression found in women with

uterine cervical carcinoma demonstrated a poor prognosis (Hedman *et al.*, 2010). Moreover, peri-nulcear staining of LRIG3 was significantly correlated with better survival of patients with astrocytic tumors (Guo *et al.*, 2006a).

2.2.2 Role of LRIG in cancers

Lately, LRIG1 has emerged as an important tumour suppressor and this notion is supported by several experiments. Epidermal growth factor receptor family is well known for its putative function in cancers. LRIG1 was found to co-immunoprecipitate and downregulate all four members of the ERBB receptor family (Laederich *et al.*, 2004). In addition, LRIG1 physically interacts with EGFR via its ectodomain and recruits E3 ligase through a CBL binding domain in LRIG1's intracellular domain. Subsequently, EGFR is ubiquitylated and degradated at an increased rate as shown in figure 2.3 (Gur *et al.*, 2004). Further, there was a marked reduction in EGFR degradation in cells which expressed mutated EGFR Cbl-binding site (Y1045F) and LRIG1 lacking the Cbl-binding site. LRIG1 also downregulates EGFR in Cbl independent manner though the exact mechanism not yet known (Stutz *et al.*, 2008).

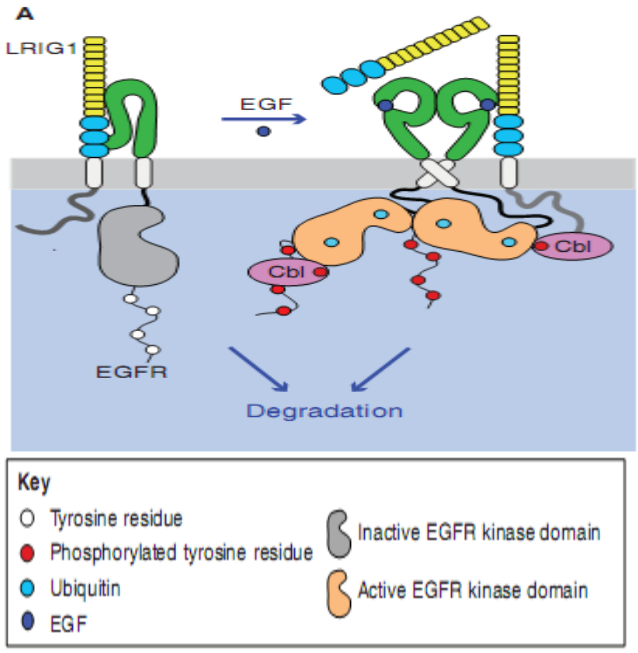

Figure 2.3: Mechanism of EGFR inhibition via LRIG1. LRIG1 Cbl domain physically interacts with activated EGFR and directs EGFR ubiquitylation. Moreover, LRIG1 can also lead degradation of inactivated EGFFR via unknown mechanism adapted from Segatto *et al.*, 2011.

Moreover, germline deletion of LRIG1 lead to increased levels of EGFR receptors in intestine. In another study, LRIG1 deletion resulted in enhanced EGFR signaling in keratinocytes (Suzuki *et al.*, 2002; Powell *et al.*, 2012). Gene silencing of LRIG1 in human glioma showed profound proliferation and invasion (Mao *et al.*, 2012). In addition it was observed that LRIG1 inhibits proliferation in cancer cell including human embryonic kidney-293 cells and bladder carcinoma cells (Jensen *et al.*, 2006; Yang *et al.*, 2006; Gur *et al.*, 2004; Laederich *et al.*, 2004). Moreover, LRIG1 associates with other tyrosine kinase receptors including RET and MET thus, it

appears that LRIG1 has a key role in controlling cell growth. Latest in vivo experiments demonstrated development of duodenal adenomas in LRIG1-/- mice (Powell *et al.,* 2012). LRIG1 locus has been found deleted and mutated in nasopharyngeal (Sheu *et al.,* 2009), renal (Willers *et al.,* 1996), colorectal, glioblastoma and breast cancers (Maitra *et al.,* 2001; (The Cancer Genome Atlas; see Experimental Procedures). In lung, colon and prostate cancer cells transcriptional expression of lrig1 was found to be low as compare to the normal tissues. (Hedman *et al.*, 2002).

In context to LRIG2 and LRIG3, their roles in cancer are least studied so far. However, recent study showed that downregulation of LRIG2 decreased activation of EGFR signaling and proliferation in glioblastoma cells. This appears that LRIG2's cytoplasmic domain recruits other protein rather Cb-1 which stabilizes the EGFR and hence enhances its activity (Wang *et al.*, 2009). LRIG3 is most homologous to LRIG1. LRIG3 was found to increase receptor expression when it was ectopically expressed (Abraira *et al.*, 2010). However, in human glioblastoma cell line (GL15) as a result of LRIG3 knocked down EGFR expression was only slightly increased (Cai *et al*, 2009). Thus, further studies are needed to elucidate role of LRIGs in cancers.

2.3 LRIG1 REGULATES EPIDERMAL STEM CELL QUIESCENCE

Mammalian epidermis consist interfollicular epidermis (IFE), hair follicles (HF), sebaceous glands (SG), and sweat glands and they contain stem cells distinguished on the basis of cell surface markers (Owens *et al*., 2003). Several signaling pathways including Notch, EGFR and Wnt regulate proliferation of stem cells in IFE **(**Schneider *et al*., 2008; Panelos *et al*., 2009; Blanpain *et al*., 2009). Recently, LRIG1 was found as a marker of interfollicular epidermal stem cells. Despite the EGF stimulation, cells expressing LRIG1 showed no response and resulted in stem cell quiescence thus LRIG1 regulates stem cell quiescence in epidermis (Jensen *et al*, 2009). Loss of LRIG1 had no effect on HFs and SGs however; hyperproliferation in IFE was profound (Jensen *et al*, 2009). Further, studies based on lineage map analysis revealed LRIG1 as a marker of both small intestinal and colonic stem cell population (Powell *et al*, 2012). These findings imply that LRIG1 has a key role in the maintenance of tissues that are under vicious cycle of self-renewal.

2.4 ROLE OF LRIG IN PSORIASIS

Psoriasis is a skin disorder affecting people globally. Psoriasis is a T cell mediated autoimmune disease which leads to hyperproliferation of keratinocytes. It is caused by genetic factors and aggravated by certain stimulating factors however, the exact mechanisms which define the severity of the disorder are unknown (Raut *et al*., 2013). Psoriasis can occur at any age however, it is mostly diagnosed before the age of 40 (Henseler *et al*., 1985). There are different types of psoriasis, psoriasis vulgaris is

the most common type and then there is an acute type of psoriasis known as guttate psoriasis which resolves within 3 to 4 months (Griffiths *et al.*, 2007). Interestingly, psoriasis is also associated with systemic disorders such as arthritis, obesity, diabetes and Chron's disorders (Henseler *et al.*, 1995; Yates *et al.*, 1982; Ruiz *et al.*, 2012).

The epidermis, the outer most layer of the skin which protects us from the environment, consists several different layers: the basal layer, spinous layer, granular layer and the cornified layer (Blanpain *et al.*, 2009). In the basal cell layer, epidermal stem cells are responsible for the constant renewal of keratinocytes, which constitute the majority of the cells in the epidermis. In the basal cells, epidermal stem cells continuously divide, migrate and differentiate as they move to other layers and mature in to keratinocytes (Blanpain *et al.*, 2009). In case of psoriasis, the epidermis layer becomes thick due to hyperproliferation of keratinocytes, the rate of migration of keratinocytes from the basal layer to the cornified layer is reduced from 40 days to 6-8 days in psoriatic skin and keratinocytes are less differentiated (Tomic *et al.*,1998). In addition, there is an increase in inflammation and inflammatory cells such as T cells and dendritic cells (Chamian *et al.*, 2004).

Epidermal growth factor receptor (EGFR) is expressed in the epidermis (Nanney *et al.*, 1984). It plays a pivotal role in keratinocyte proliferation and survival, inhibition of differentiation, cytokine secretion and wound healing (Crew *et al.*, 1933). In addition, genetically modified mice which over expressed amphiregulin an EGFR ligand developed Psoriasis-like phenotypes (Nanney *et al.*, 1984). Moreover, LRIG-1 -

/- mice histopahological features suggested its resemblance with psoriasis epidermis: the epidermis became thick with increased proliferation but altered growth and differentiation of keratinocytes and with increased infiltration of neutrophils (Wong *et al.*, 2012). Further immunohistochemical analysis demonstrated that LRIG-1 protein was highly expressed in epidermal basal cells and hair follicle cells in the normal mouse-tail skin however; the expression was decreased in psoriasis skin (Wong *et al.*, 2012). Thus, this suggests that LRIG-1 regulates the proliferation of epidermal keratinocytes but the exact mechanism involved is unknown.

2.5 EPIDERMAL GROWTH FACTOR FAMILY OF RECEPTOR

The EGFR also known as ErbB-1/HER1, along with ErbB-2 (HER2), ErbB-3 (HER3) and ErbB-4 (HER4) belong to ErbB family of receptor tyrosine kinases (RTK) (Ferguson *et al.*, 2003 and Yarden, 2001). EGFR was the first member of the family to be identified as a binding partner of EGF which regulated eyelid opening in mice. Later, it was found that mutated EGFR impairs mammary gland development (Cohen, 1997; Carpenter *et al.* 1978). So far, EGFRs and its ligands have been demonstrated to play a key role in embryonic development and tissue renewal. In addition, these receptors are over expressed and mutated in various human cancers and are a target for anticancer drug development (Suzanne, 2011). These receptors are encoded by four receptor genes: EGFR/erbB-1, c-erbB-2/HER2, c-erbB3-/HER3 and c-erbB4/HER4 which are alternatively spliced to give rise to numerous protein products (Robinson *et al.*, 2000). Furthermore, these receptors are activated by 13 ligands including Epidermal growth factor (EGF), transforming growth factor-α (TGF-

α), HB-EGF (heparin binding), beta-cellulin, amphiregulin (AREG), epiregulin, epigen (EPG), betacellulin (BTC) and the neuregulins (NRGs) 1–4 *(*Olayioye *et al*.. 2000). Most of these ligands are initially expressed as membrane-anchored proteins that require proteolytic cleavage either to achieve activity in solution or bind to cell surface proteoglycans acting as reservoir and are available when needed. (Falls, 2003). Where, EGF and TGFα are the well known EGFR binding ligands and NRGs preferably bind with ErbB-3 and ErbB-4. However, BTC bind and activate all receptors (Higashiyama *et al*., 2008).

2.5.1 Structural features of EGFR family and downstream signaling

All Erb-B receptors contain glycosylated, extracellular ligand binding domain which consists of two homologous ligand binding sites: L1 and L2. In addition, it contains two cysteine-rich domains S1 and S2 of which S1 is involved in EGFR dimerization (Garrett *et al*., 2002; Ogiso *et al*., 2002). Further, the kinase activity is mediated by highly conserved SH1 domain present in the cytoplasmic region. This region also contains six tyrosine residues available for transphosphorylation. Moreover, the extracellular domain and the intracellular domain are connected via a transmembrane region as depicted in figure 4 (Bazley., 2005).

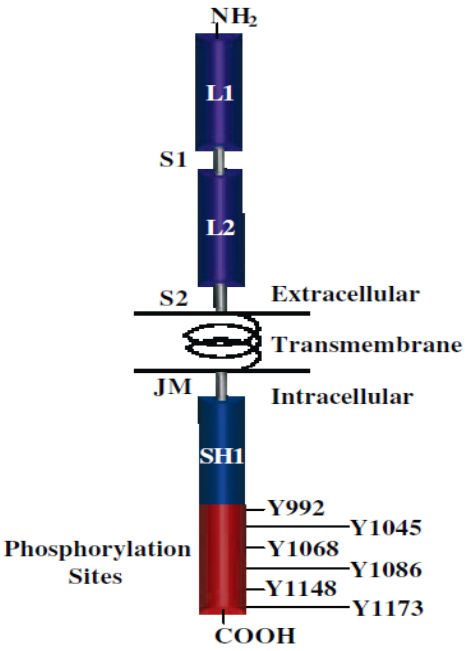

Figure 2.4: Structural representation of EGFR family showing extracellular, transmembrane and intracellular membrane with six its phosphorylation sites adapted from Bazley, 2005

These receptors in an inactive state without the presence of a ligand show a monomeric conformation and are evenly distributed over the cell membrane (Ferguson *et al.*, 2003). However, as soon as the ligand binds, interaction loop is exposed; receptors form either homodimers or hetrodimers and attain a stable conformation with increased ligand binding affinity. The receptor phosphorylation and internalization events ensue (Ben *et al.*, 1992). Furthermore, the phosphorylated receptors act as a docking site for various adaptor proteins and direct substrates such as Shc, Grb2, P13K, AKT, mTOR and STAT5. The major signaling pathways activated by EGFR include PI3 kinase, Ras-Raf (MAPK), JNK and PLC gamma.

These signaling systems are particular important for cell proliferation adhesion and motility, as a protection against apoptosis at the cellular level, and to promote invasion and angiogenesis at the physiological level in normal cells as shown in figure 2.5 (Suzanne *et al.*, 2011).

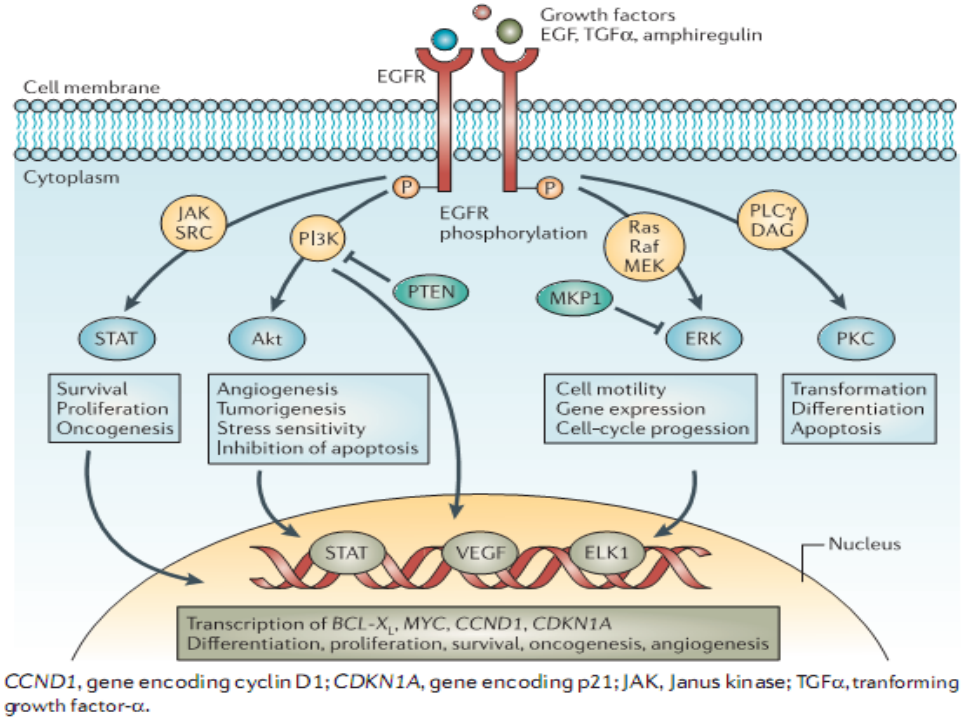

Figure 2.5: Signaling pathways activated by EGFR. Several activated downstream signaling pathways directly or indirectly via EGFR from Mukesh *et al.*, 2006.

Activated EGFR are immediately targeted by inhibitory mechanisms involving dephosphorylation by protein tyrosine phosphatases and degradation of ligand receptor complex in lysosomes via endocytosis (Keilhack *et al.*, 1998; Sorkin and Goh, 2009). In addition, activated EGFRs regulate the de novo expression of EGFR inhibitors. So

far, four inducible feedback inhibitors have been found which are LRIG1 (Gur *et al.*, 2004), suppressor of cytokine signalling 4 and 5 (SOCS4 and SOCS5) (Nicholson *et al.*, 2005) and receptor-associated late transducer (RALT) (Fiorentino *et al.*, 2000). The maximum expression of RALT, SOCS4 and SOCS5 is achieved within 60 minutes of the initial EGFR activation; however, LRIG1 expression is attainted after 3 hours of EGF stimulation (Fiorentino *et al.*, 2000; Kario *et al.*, 2005; Gur *et al.*, 2004).

2.6 EPIDERMAL GROWTH FACTOR RECEPTOR FAMILY IN CANCERS

Epidermal growth factor receptors have been found mutated and over expressed in various solid human tumors including breast, ovarian, lung, bladder, head and neck cancers (Salomon *et al* .,1995). Thus, these receptors have been widely studied over the decades.

2.6.1 Role of Epidermal growth factor receptor family in Cancers

Human tumors develop due to multistep processes comprising six biological acquired complexities which include sustaining proliferative signaling, evading growth suppressors, resisting cell death, enabling replicative immortality, promotes angiogenesis, invasion and metastasis. Interestingly, EGFRs play a significant role in promoting oncogenesis via initiating earlier mention hall marks of cancers. De Jong et al found simultaneous expression of EGFR and TGF α which was associated with microvessel density in invasive breast carcinoma (Jong *et al.*, 1998). Further, TGFα and EGF were found to stimulate angiogenesis in the hamster cheek pouch assay (Schreiber *et al.*, 1986). In addition, TGF α promotes the expression of VEGF which is

key regulator of vascular cell permeability and leads to angiogenesis (Dvorak *et al.*, 1995). Another study in consistent with these findings, showed that VEGF increases expression of heparin-binding-EGF in vascular endothelial cells and in return they promote mitogenic and chemotactic activity of mesenchymal cells thereby enhancing angiogenic process (Arkonac *et al.*, 1998).

Moreover, it was found that EGF generates anti-apoptotic signals in cells over expressing EGF receptors (Kulik *et al.*, 1997). Likewise, it was demonstrated that in the presence of EGFR tyrosine kinase inhibitor, survival and proliferation of HN5 and colorectal cancer cell lines increases (Moyer *et al.*, 1997; Karnes *et al.*, 1998). Additionally, Moyer et al also found that EGFR inhibitor promotes accumulation of unphosphorylated retinoblastoma protein (RB) and Cyclin-dependent kinase inhibitor 1B (p27KIP1) which arrests DiFi human colon tumour cells at G1 phase (Moyer *et al.*, 1997). Last but not the least; EGFR mRNA expression was upregulated in highly metastases human colon cancer cells (Radinsky *et al.*, 1995). Further, tumour invasiveness was found to be associated with EGFR-positive gastric carcinomas (Prakash *et al.*, 1997).

2.6.2 EGFR as prognostic markers

Salomon et al have extensively reviewed various tumors expressing high levels of EGFR and found a correlation with enhanced metastases, poor prognosis and low patient survival (Salomon *et al.*, 1995). Likewise, numerous other studies have demonstrated consistent findings, few have been stated here:

A study in transitional cell carcinoma of the bladder revealed that EGF and TGF-α expression correlated with tumor recurrence (Turkeri *et al.*, 1998). In breast cancer, EGFR-negative tumor patients showed increased survival as compare to patients with EGFR-positive tumors (Bucci *et al.*, 1997). Moreover, a study of 142 breast cancer, EGFR expression was associated with advanced, axillary lymph node status, and histological grade (Beckmann *et al.*, 1996). Similarly, EGFR positive carcinomas were found to correlate shorter survival and impaired response towards to chemotherapy with platinum compounds (Fischer *et al.*, 1997).

2.7 WOUND HEALING

The process of wound repair is divided in three stages: inflammation, new tissue formation and remodeling phase. Inflammation phase lasts for 48 hours post injury. The environment of the wound is hypoxic with abundant fibrin clot, Bacteria, neutrophils and platelets (Grose and Werner, 2004). Then is the new tissue formation phase which starts from day 5 to day 10 after injury. New blood vessels are formed with capillaries associated fibroblasts and macrophages which substitute the fibrin matrix with granulation tissue. In addition, keratinocytes proliferate and mature and form a new epithelium layer. There are few growth factors which promote angiogenesis such as vascular endothelial growth factor A (VEGFA) and fibroblast growth factor 2 (FGF2) (Werner and Grose, 2003). Angiogenesis can also occur by the recruitment of bone-marrow-derived endothelial progenitor cells (Bluff *et al.*, 2007). Later, fibroblasts are recruited from the edge of the wounds by macrophages, few mature in to myofibroblasts and contracts the wound (Opalenik *et al.*, 2005).

Moreover, Fibroblasts and myofibroblasts produce extracellular matrix which form a scab (eschar) on the surface of the wound (Krieg, *et al.*, 2007).The last phase is the remodeling phase which occurs about 12 months after repair. The re-epithelialized wound is raised than the surrounding surface; new collagen has been laid by fibroblasts however the healed region lacks normal appendages as shown in figure 2.6.

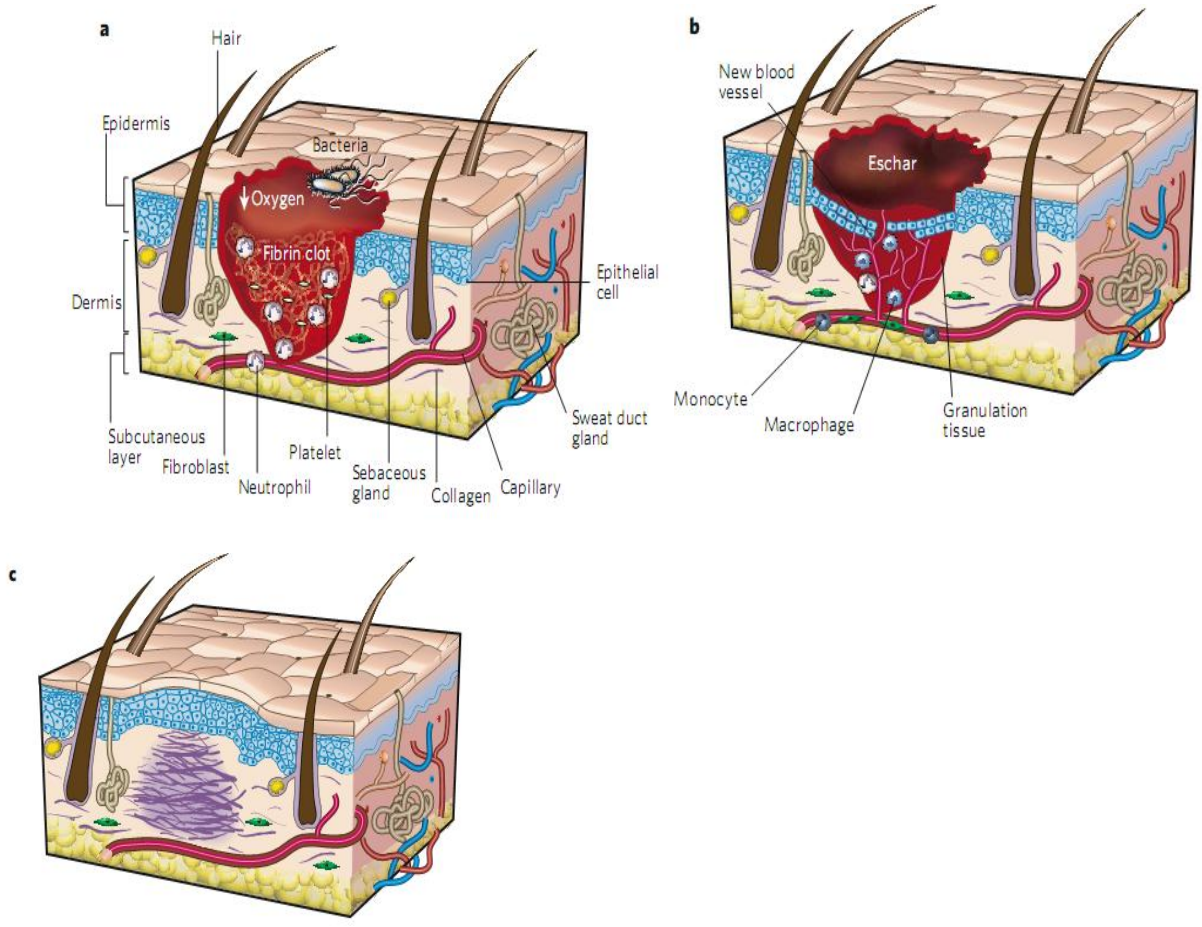

Figure 2.6: The three classical phases of wound repair: (a) Inflammation (b) New tissue formation (c) Remodelling adapted from Gurtner et al., 2008.

2.7.1 Mechanism of EGFR activation during re-epithelization phase

The re-epthelization phase during the first 3 days (Pastore *et al.*, 2008), angiotensin II and catecholamines induce keratinocyte and fibroblast migration via G protein coupled (GPC) angiotensin II receptor. Followed by initiation of metalloproteinase (MMP)-mediated shedding of EGFR ligands which lead to EGFR activation (Yahata *et al.*, 2006; Pullar and Isseroff, 2006). It was recently found that EGFR mediated ERK pathway can also be activated by both TNF-α and IFN-γ (Mascia *et al.*, 2003). Moreover, Integrins additional physical complexes at the cell membrane activate EGFR via ligand-independent mechanisms as shown in figure 2.7 (Cabodi *et al.*, 2004).

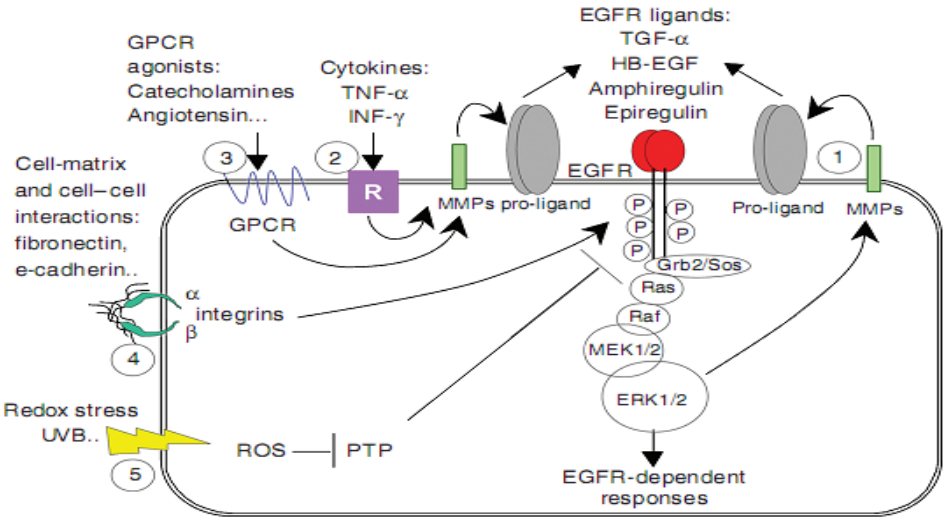

Figure 2.7: Mechanism of EGFR activation in keratinocytes adapted from Pastore *et al.*, 2008.

In *vitro* studies have shown that the activation of EGFR enhances on the induction of a ligand, followed by epithelial migration after wounding (Hudson and McCawley, 1998). Further, a study was conducted to directly determine the significance of endogenously expressed EGFR on keratinocyte migration following incisional wounding in EGFR null and wild-type control mouse skin. EGFR induced proliferation of keratinocytes was highest on day 1 and least on day 5 in EGFR wild type mice. In EGFR null mice it was found to be least on day 1 with highest on day 5 however, the maximum number of keratinocytes were less in comparison with EGFR wild type mice (Repertinger *et al.*, 2004).

2.8 WOUND IMPAIRMENT IN DIABETES

Diabetes affects about 170 million people globally which is predicted to double in future. These patients suffer from several complications including diabetic foot ulcers. It is estimated that 15% of all diabetic patients suffer from foot ulcers (Reiber *et al.*, 1999). In situations where patients with diabetes suffer a break in the skin of their foot, lack an ability to fight infection and to initiate an appropriate inflammatory response. Thus, the site of wound becomes prone to infections that can lead to sepsis or may require limb amputation. Moreover, there are several physiologic factors which lead to impaired wound healing these includes reduced expression of growth factors such as platelet-derived growth factors, vascular endothelial growth factors and EGF receptor, insulin-like growth factor-1 (Galkowska *et al.*, 2006). In addition, low level of angiogenic responses, reduced granulation tissue (Falanga, 2005) and restricted

keratinocyte and fibroblast migration and proliferation (Gibran *et al.*, 2002) (Figure 2.8)

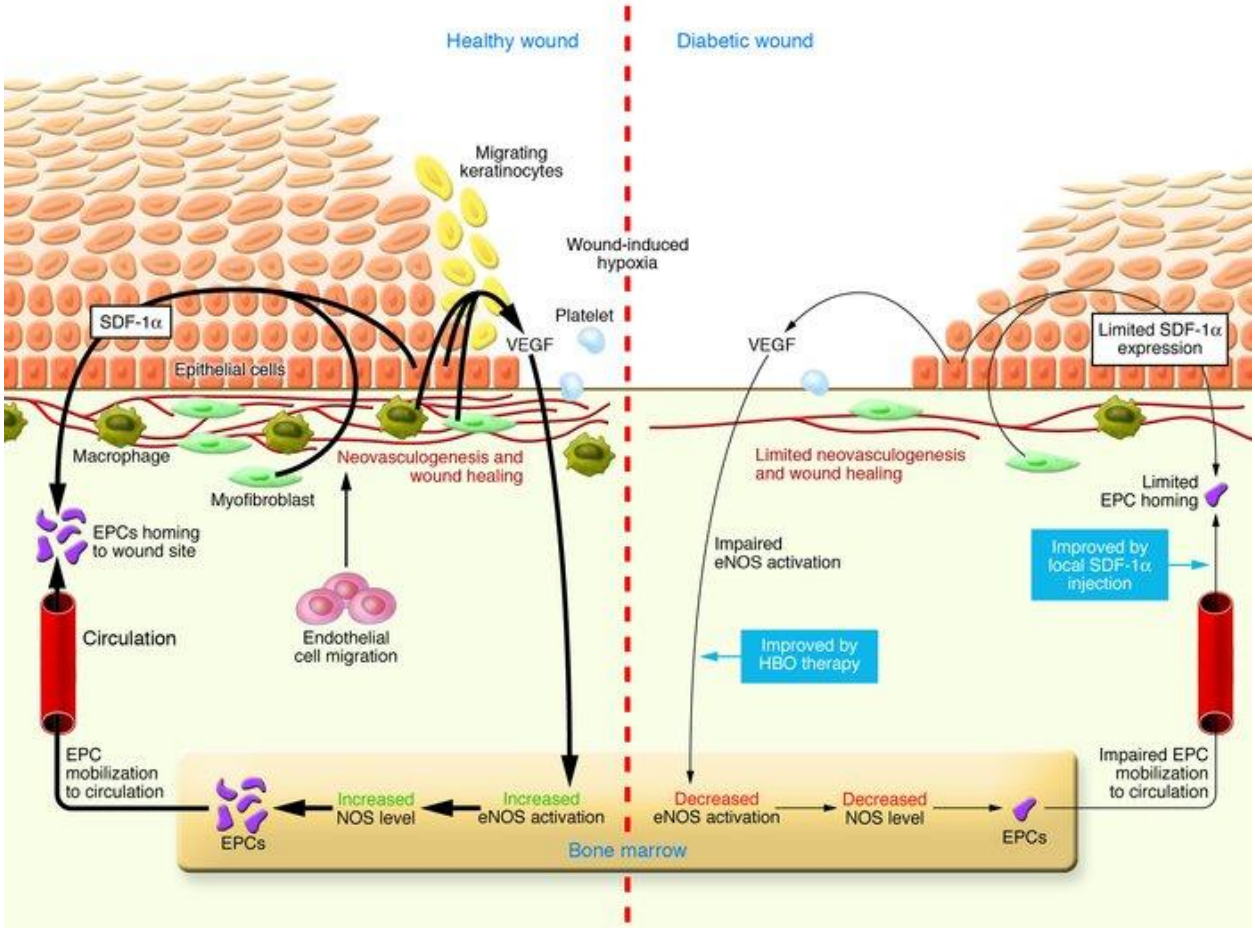

Figure 2.8: Comparison of wound healing mechanism in healthy individuals with diabetics. The acute wounds in healthy individuals are regulated via induction of several cytokines and chemokines. In the presence of wound induced hypoxia, where macrophages, fibroblast and epithelial cells release VEGF which phosphorylates and activates eNOS in the bone marrow, triggering an increase in NO levels. Then, bone marrow epidermal progenitor cells (EPCs) are mobilized to the circulation. Further, chemokine SDF-1α recruits the homing of these EPCs to the site of wound, where

they cause neovasculogenesis. However, in Diabetic patients there is reduced eNOS phosphorylation and SDF-1α which directly affects EPCs homing at the site of injury from (Brem and Tomic, 2007)

2.9 CYCLIN DEPENDENT KINASE (CDK) INHIBITOR P27 (KIP1)

Cyclin dependent kinase inhibitors are divided in two major families: CIP/KIP and INK4 on the basis of sequence similarity and CDK targets (Sherry, 1999). INK4 family of protein inhibitors includes p15, p16, p18 and p19, they share approximately 40% homology with one another (Roussel, 1999). Each varies between 15 to 19kDa and contains four to five ankyrin repeats, which specifically bind and inhibit CDK4, CDK6 and D type cyclins (Noh, 1999). In contrast, CIP/KIP family of protein inhibitors is composed of a 65 amino acid conserved motif at amino terminal which allows them to bind with cyclin D, A and B dependent kinases (Chen *et al.*, 1995). Moreover, they all have a nuclear localization signal at carboxyl terminal domain. P27 along with p21 and p57 belong to CIP/KIP family of inhibitors (Wade *et al.*, 1993; Polyak *et al.*, 1994; Matsuoka *et al.*, 1995; Nakanishi *et al.*, 1995). P27 interacts with cyclin-cdk2 complex and has separate binding sites on cyclin and cdk subunits. P27 consists, ten amino acids long rigid coil, having LFG motif (Leu, Phe, Gly sequence) which is conserved in all KIP/CIPS family members and provides partially extended conformation as it binds to shallow groove formed by alpha1, alpha2 and alpha 3 helices of cyclin-box repeat of cyclin A. This peptide binding groove consists of

hydrophobic amino acids which are conserved in cyclin family that allows different CDK complexes to interact with p27 (Alicia *et al.*,1996). Further, p27-cdk2 interaction involves three consecutive structural elements of p27, β hairpin, β strand and 310 helix. Although they all make an impact in bringing conformational changes in cdk2, however, the key inhibitory effect occurs when 310 helix of p27 (residues 85-90) binds with the catalytic cleft of cdk2 and occupies all the available space, which would lead to reduced affinity for ATP (Alicia *et al.*,1996). This notion was consistent with a finding which demonstrated that truncated form of p27, lacking 310 helix losses most of its inhibitory activity (Luo *et al.*, 1995; Polyak *et al.*, 1994).

2.9.1 Role of p27 in cancers

P27 is recognized as a tumor suppressor, mediator of apoptosis, key regulator of cell differentiation and controls drug resistance in solid tumors. However, P27kip1 is well known for its putative function which is it acts as a cyclin dependent kinase inhibitor. During early G1 phase, the cyclin E/CDK2 and cyclin A/CDK2 complexes are sequestered by p27KIP1. In response to mitogens, cyclin D expression increases and which then form complexes with CDK4 or CDK6 and p27KIP1. As a result, cyclin E is no longer bound to p27KIP1 and is free to phosphorylate RB. Thus, cell exits G1 and enters S phase.

Two different mechanisms have been inferred to be involved in p27 inactivation during tumour development: its nuclear export and enhanced protein degradation. During G1–S transition, p27 is actively phosphorylated at Thr187 by cyclin E-CDK2

(Muller and Morris, 1989) Thr187-phosphorylated p27 is recognized by Skp2-containing E3 ubiquitin ligase, SCF, and its cofactor, Cdk subunit1 (Cks1) and which promote its degradation by proteasome (Carrano *et al.*, 1999). However, p27 sub cellular localization is dependent on phosphorylation of three key amino acid residues S10, T157, T198. Phosphorylation at S10 is accomplished by Human kinase interacting stathmin (hKIS) and AKT which facilitate p27 nuclear exclusion (Rodier et al., 2001). P27 contains a putative Akt consensus phosphorylation site (RXXRXXT157D) in its nuclear localization sequence (NLS; amino acids 151–166). Shin I et al experimental studies showed that p27 is phoshosphorylated at Thr157 by Akt (Shin *et al.*, 2002). Further, NLS also contains a site which when recognized by a complex of importin α3, importin α5 and importin β aids p27kip1 transportation via nuclear membrane. However, AKT1 dependent phosphorylation at T157 promotes its binding with 14.3.3 instead of importin complex. Thus, results in cytoplasmic retention of p27, which impairs its CDK2 inhibitory activity and role in cell-cycle progression (Toshihiro *et al.*, 2004). In addition, this mechanism is exploited by breast cancer cells whereby AKT1 induced T157 phosphorylation leads to p27 mislocalization and its suspension of cell cycle arrest (Viglietto *et al.*, 2002). However, mutation at T157 impedes AKT1 induced phosphorylation and its subsequent outcomes. In addition AKT1 also phosphorylates p27 at T198. Furthermore, as with T157, phosphorylation at T198 is increased in breast cancer cell lines as compared to normal mammary epithelial cells and both cause cytoplasmic retention of p27 via promoting binding with 14-3-3 (Toshihiro *et al.*, 2004). Moreover,

experiments have demonstrated complete reversion of AKT1 induced cytoplasmic relocalization only in the presence of double mutation at T157A and T198A (Motti *et al*., 2004). Interestingly, epithelial cancers which over express EGFR show increased p27 proteolysis. In addition, inhibition of EGFR by gefitinib regresses EGFR mediated p27 degradation (Chu *et al*., 2008). However, the pathways that drive p27 degradation are not yet known.

Thus, their role in cell cycle justifies them to be known as a tumour suppressor and that any alteration in functionality of these proteins will ultimately lead to uncontrolled proliferation of the cells. In accordance, numerous gene deletions in p15 and p16 have been found in various human tumors. A germline mutation in P16 gene was identified familial melanoma patients (Hussussian *et al*., 1994). Moreover, p16 and p15 was found homozygously deleted in brain tumors (Jen *et al*., 1994) depicting that inactivation of CDKIs play an important role in some tumors. P27Kipl has been mapped on the chromosome 12 which is known to contain deletions and rearrangements in leukemia and mesotheliomas. Norihiko et al, Veronica and Castaneda et al in independent studies found neither deletions nor rearrangements in p27 gene when screened in various soild tumors (Kawamata *et al*., 1995; Ponce *et al*., 1995). However, a hemizygous deletion in p27 was found in a B-cell non-Hodgkin's lymphoma (Morosetti *et al*., 1995). In adult T-cell leukemia, a stop codon mutation at 76 was found (Morosetti *et al*., 1995). In addition two point mutations were found during 36 primary breast carcinomas. One of the mutations in the breast carcinomas

was a polymorphous mutation at codon 142 and the other a nonsense mutation at codon 104 (Spirin *et al*., 1996).

Chapter 3

MATERIALS AND METHODS

3.1 BUFFER STOCKS AND SOLUTION RECIPES

3.1.1 Formalin Solution (10%, buffered neutral)

In 500ml of distilled water, 100ml of Formaldehyde (37-40%), 4 grams of NaH2PO4 and Na2HPO4 (anhydrous) 6.5 grams were added. Solution was mixed until all salts were dissolved and volume was adjusted to 1L with distilled water.

3.1.2 10X PBS

To prepare 1000 ml of 10X PBS, 80 grams of NACL, 2 gram of KCL, 14.2g of NA2HPO4 and 2.45 grams of KH2PO4 were added in a conical flask and 800 ml of distill water was added. The Ph of the solution was adjusted to 7.4 by addition of HCL and the volume of solution was adjusted to 1000 ml with distill water.

3.2 ANIMALS

All experiments were performed in accordance with the rulings of the Institute of Laboratory Animal Research, Division on Earth and life sciences National Institute of Health, USA (guide for the Care and Use of Laboratory Animals: Eight edition, 2011). A total of 20 Female Balb/c mice (16 weeks old, weighing 40-45gm) were purchased from National Institute of Health (NIH) Islamabad. Mice were housed in an isolated room at the animal facility of Atta-ur-Rahman School of Applied Biosciences (ASAB), NUST. The study was conducted under controlled environmental conditions;

temperature was kept between 25± 2 degrees with natural light and dark cycles (14 hour of night and 10 hours of day). Mice which were to be sacrificed on the same day were grouped and kept in the same cage; all mice had equal access to food and water.

3.3 STUDY TIMELINE

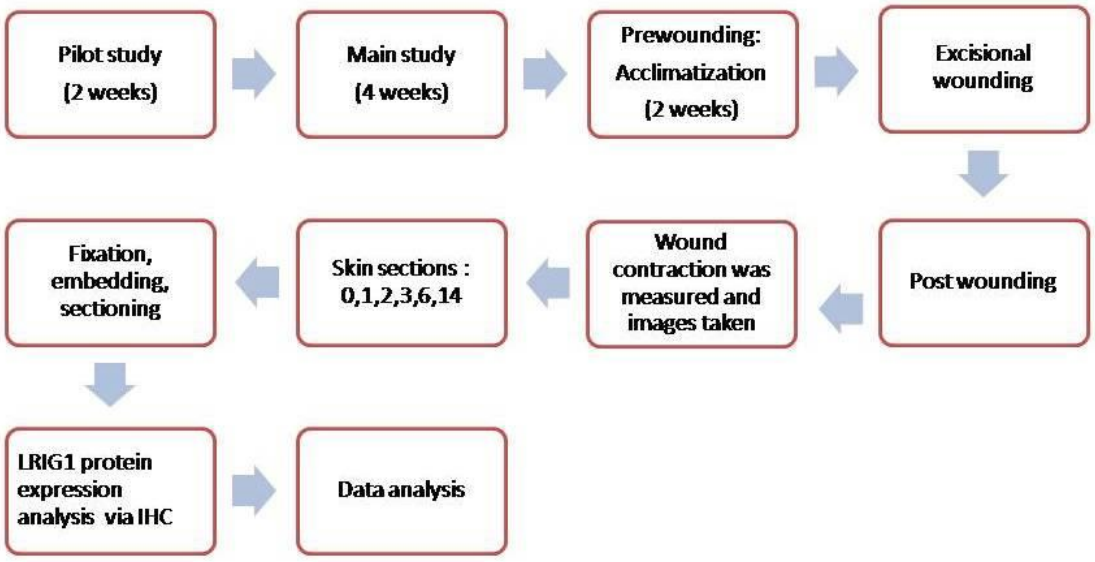

3.4 EXCISIONAL WOUNDING

Mice were held from the neck directly behind the ears and the tails were grasped while their heads down. Freshly prepared anesthesia a combination of (Ketavet (ketamine)/Rompun (xylazine) was injected in the intraperitoneal cavity. After 5 to 10 minutes mice became unconscious until then they were kept in the cage. The back of the anesthetized mice were shaved with an electric razor and the remaining hairs were removed with hair removal cream. The skins were held with forceps and full thickness

cutaneous layers were excised with 5mm wound biopsy punch. Each mouse was given two wounds.

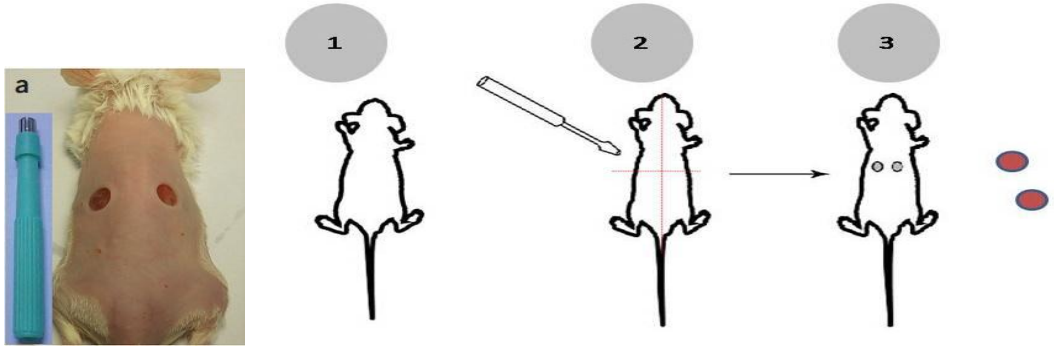

Figure 3.1: Excisional wound healing model a three step process. A Shown punch wound biopsy instrument and excisional wounded mice. B Three step process for excisional wounding, in first step hairs are removed. Second step, the dorsal surface of the mouse was divided in four quadrants, then full thickness cutaneous layer was excised from each quadrant via biopsy punch.

3.4.1 Progression of wound healing

Days: 0, 1, 2, 3, 6 & 14 were selected by referring an earlier study demonstrating EGFR expressions on the following days (Repertinger *et al*., 2004). The digital images of the wounds were taken with 12x digital camera on these days. It was ensured that the wound was healing properly and the mice were not scratching their own wounds. Further the area of the wounds was measured by measuring length and width of the wounds by vernier caliper. Percentage of the wound contraction for the earlier mentioned days was measured by the formula : area of original wound – area of the actual wound /area of original wound x 100 adapted from Wang *et al* ., 2013

3.4.2 Collection of wound specimens

Mice were sacrificed on the predetermined time points mentioned in study timeline. Mice were sacrificed on designated days through cervical dislocation. During cervical dislocation the disruption of fragile dorsal skin tissues were avoided especially on day 3 and 6 post wounding. The animals were declared dead after checking their palpations. Later, 2mm of skin adjacent to wound margin along with 5mm of wounded tissues were excised using scissors, lifted by forceps and the hanging granulation tissues were carefully removed. Each excised wound tissue was bisected and was kept flat, upright position in histology cassettes which was then dipped in 4% formaldehyde at 4 degrees overnight for fixation.

3.4.3 Tissue fixation

Tissue were fixed in 10% buffered formalin with neutral PH and kept at 4 degrees overnight. Tissues were fixed chemically to prevent bacterial induced decomposition of the samples and to make them suitable for processing, cutting and staining.

3.4.4 Tissue processing

To prepare thin sections a solid block of tissue was prepared by tissue impregnation. Impregnation of tissue supports the tissue and avoids breakage of tissue during tissue sectioning. Before impregnation, tissue was processed by the following steps:

1. Dehydration:

   Water contents were removed from the samples by treating them with 70% isopropanol for one hour, 90% isopropanol. Later tissues were dipped in absolute isopropanol.

2. Clearing:

   Samples are dipped in xylene for one hour.

3. Impregnation:

   In this step xylene was removed and substituted with paraffin wax. Tissues were kept in paraffin wax at 54 to 60 degrees.

3.4.5 Tissue embedding

Embedding molds were filled with melted paraffin and with the help of the forceps, tissue were pressed down in mold. Proper orientations of the skin samples were ensured. The samples were placed in cryo-console to maintain cold temperature.

3.4.6 Microtomy of paraffin blocks

The blocks were roughly cut to 10 -15 microns in order to expose the tissues in one plane. Then Formalin-fixed paraffin-embedded tissues were sliced by microtome in to 5µm thick sections and mounted on glass slides. Later samples were fixed on the slides by incubating for one hour at 70 degrees on a heat block.

3.5 HEMATOXYLIN AND EOSIN STAINING

The tissues were cleared of all wax and were rehydrated to allow the entry of basic dyes (hematoxylin) and acidic dye (eosin). The tissues sections were dipped in xylene for 3 min, then in absolute alcohol for 3 min. Later samples were placed in 70% alcohol for 2 min and then washed by water. Samples were exposed with hematoxylin for 3 to 5 minutes. The dye was washed with water for 30 seconds followed by removal of excess dye by continuous agitation in 1% acid alcohol for 15 seconds. The samples attained a blue colour after 2 to 3 dips in ammonia water. The samples were counter stained with eosin for 2 to 3 minutes. Lastly, samples were dehydrated by passing them first in 75% alcohol and then in 95% alcohol.

3.6 IMMUNOHISTOCHEMISTRY

Immunohistochemistry technique is used to detect distribution and localization of a specific protein (antigen) via specific antibody. As soon an antibody-antigen reaction occurs it is visualized by fluorescent dye, enzyme, radioactive element or colloidal gold. Either, frozen sections or paraffin embedded sections tissues are applicable for immunohistochemical techniques. Although antibody is highly specific there are chances that it can bind nonspecifically. Therefore, in order to ensure that only protein of interest was visualized, negative and positive controls were used during protocol optimization phase. For positive control ideal conditions were used. Besides a positive control a negative control was preceded along with it but the difference is that the section was not incubated with primary antibody.

3.6.1 Deparaffinzation

Glass slides were mounted on a plastic slide holder and dipped in 100% xylene for 20 minutes in order to remove residual paraffin from the samples.

3.6.2 Rehydration

Samples were rehydrated in a series of steps, which are as follows:

Washed slides in 100% ethanol for 10 min

Washed slides in 90% ethanol for 10 min

Washed slides in 70% ethanol for 5 min

Washed slides in 50% ethanol for 3 min

Washed slides in 30% ethanol for 3 min

Rinsed slides in running distill water for 2 min

The samples were observed as white discs on the glass slides as soon as they were dipped in water. Henceforth all steps were kept in humidity chamber to avoid drying which can provoke non specific background staining.

3.6.3 Blocking

To block the non specific binding of antibodies the glass slides were treated with hydrogen peroxide for 30 min. Then the slides were placed on a covered tray with tissue paper soaked with water to provide moist environment to the samples. Samples

were then washed with 1X PBS to remove blocking solution for 15 min. The samples were then covered with 10% BSA blocking agent for 10 min, which was drained off.

3.6.4 Primary Antibody Incubation

The primary antibodies anti LRIG1 (ab36707, Abcam UK) were diluted to 1/75 concentration in 1% BSA/PBS prepared by mixing 1 g of BSA in 100ml of 1x PBS. Samples were completely covered with freshly diluted antibody and then kept in humidity chamber for overnight incubation at 4 degrees.

3.6.5 Secondary Antibody Incubation

Samples were washed with 1x PBS to remove primary antibody. The HRP labeled secondary antibody (ab6721, Abcam UK) was diluted to 1/50 in 1% BSA and applied to the samples. Slides were kept in humidity chamber for 1 hour at room temperature.

3.6.6 Detection

The samples were again washed with 1% PBS to remove unbound secondary antibody. To visualize the antigen through HRP label, DAB substrate were used from Abcam DAB staining kit (Abcam Cat: ab64238, UK) which imparted an intense brown colour to the HRP labeled protein. A mixture of DAB substrate and DAB chromogen was prepared and was applied to the samples. Then the samples were incubated for 5 -10 min at room temperature after which the stain was washed with tap water. Then the samples were stained with hemotoxylin which stained the nuclei of

the cells. Samples were washed to remove the stain. Followed by dehydration of the samples by the following steps:

50% ethanol 5 min

90% ethanol 5 min

100% ethanol 5 min

Xylene 5min

The slides were mounted with a suitable mounting media and were covered with cover slips.

3.6.7 Evaluation of immunohistochemical findings

The blind evaluation of each slide was carried out independently by a pathologist. All staining were proceeded with negative and positive controls. The significance of positive and negative controls is mentioned earlier in section 3.6. Positive staining was defined as brown staining. Whereas, negative control demostrated no brown staning. Staining was observed in different skin compartments including epidermis, dermis, hairfollicles and sebaceous glands. Further it was noted whether the staining was localized in nucleus, perinucleus or in cytoplasm. On the basis of intensity of staining the LRIG1 expression was scored (as shown in figure 3.2) on the scale of 1-4:

Score 1: very low

Score 2: low

Score 3: moderate

Score 4: high

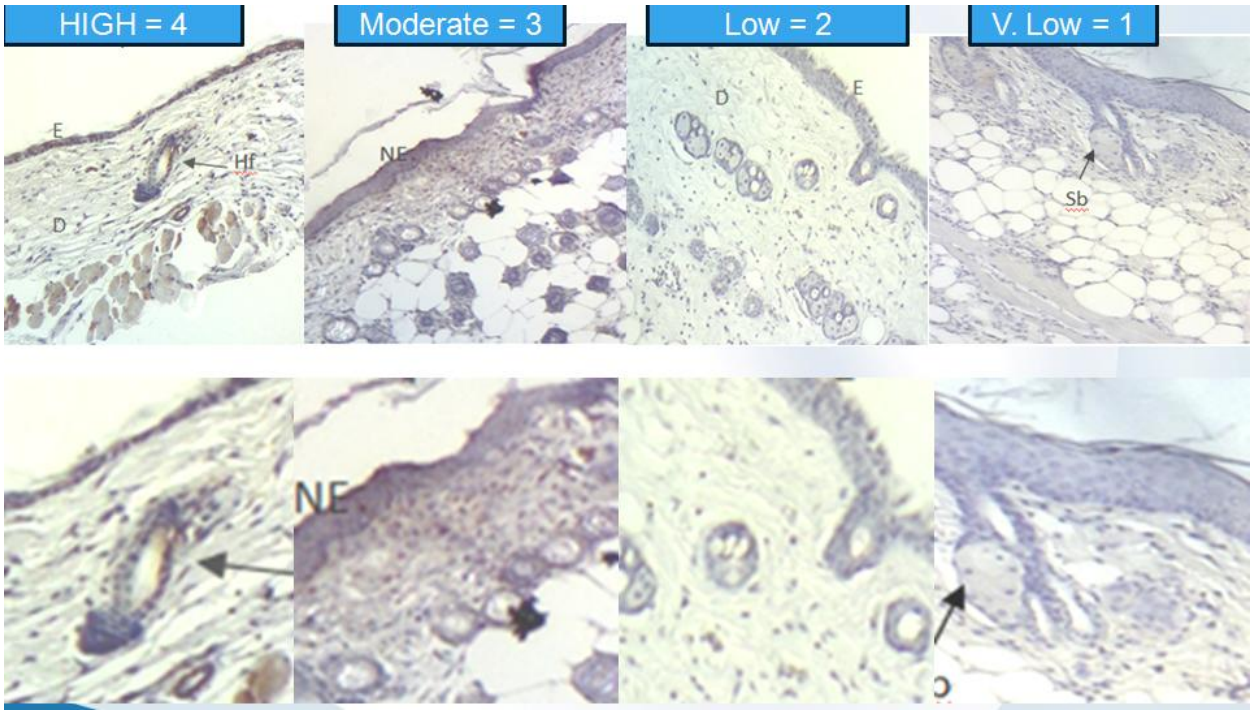

Figure 3.2: LRIG1 expressions were scored on the basis of intensity. The most intense was given a score of 4 and the least intense brown color was given a score of 1.

3.7 P27 MUTATIONAL ANALYSIS

Sequencing was retrieved from sense and antisense primers and sequence was submitted in Genebank (http://www.ncbi.nlm.nih.gov/genbank) with an accession number JX628784 by a former lab collogue. All existing human CDKN1B protein sequences were retrieved from uniprot (http://www.uniprot.org/) and were aligned to generate a wild type consensus sequence by CLC work bench (www.clcbio.com). The wild type protein sequence was aligned with our generated sequence and then sequence was analyzed for probable mutations. Later, C terminal end of the wild type

p27 protein sequence was aligned with sequences of CDKN1B orthologs present in uniprot (IDO no**:** H2Q5H2, P46414**,** Q6SLL5, O19001 and Q8JIV2).

3.8 PROTEIN MODELING

Protein sequences of CDKN1B (ID no.P46527**)** and AKT1 (ID no. P31749) were retrieved from uniprot database. Sequences were submitted to NCBI provided protein specific iteration (PSI)-BLAST tool (http://blast.ncbi.nlm.nih.gov/Blast.cgi) to obtain homologous sequences of three dimensional structures available in protein data bank (PDB).

Two PDB structures including PDB codes: 1JSU (Crystal structure of p27 cyclin dependent kinase inhibitor bound to the cyclin A-Cdk2 complex determined at 2.3Å)(Russo *et al.*, 1996) and 3O96 (Crystal structure of human AKT1 with an allosteric inhibitor resolved at 2.7Å) (Wu *et al.*, 2010) have maximum sequence identity with P27 and AKT1 respectively. So for complete 3D structure of P27 protein the structure was built using ab-initio modeling techniques. P27 protein sequence was submitted in I Tasser (Iterative threading assembly refinement) (Zhang. 2008) and Phyre2 (Protein Homology/analogy Recognition Engine V 2.0) (Kelley and Sternberg, 2009). Models generated by these software's were evaluated by online servers such as ERRAT, PROCHECK, QMEAN and Z score (Benkert *et al.*, 2008; Laskowski *et al.*, 1993). However, all models showed low ERRAT, QMEAN and Z scores. In Ramachandran plot most of the residues were found in unfavorable regions. P27 sequence was submitted in other abinitio modeling servers such as Quark and Robetta.

Multiple models were generated and one target model was selected with highest ERRAT and QMEAN scores, least Z score and with favorable Ramachandran plot statistics. Mutated model was generated using the finest model obtained in earlier steps. The modeling of mutated model was performed using MODELLER (Eswar *et al.*, 2006). The energy minimizations were performed in Molecular modeling and simulation (MOE) software (Chemical computing group's MOE software, version 2013) and then analyzed using the same criteria as was used for analyzing wild type model of P27 (NMP27). Apo-AKT1 model was derived from Human AKT bound with an alloesteric inhibitor (PDB ID no. 3O96) using MOE.

3.9 PROTEIN-PROTEIN INTERACTION OF AKT AND P27

Protein protein interactions of both non-mutated and mutated models of P27 (termed as NMP27 and MP27, respectively) were studied by using High Ambiguity Driven Molecular Docking web server (HADDOCK) (haddock.science.uu.nl) (De Vries *et al.*, 2010). The webserver generates 10 clusters. Scoring is based on Haddock score, desolvation energy, Z score, RMSD value, electrostatic energy, buried surface area, restrains violation energy and van der waals energy. Possible active and passive residues of NMP27, MP27 and AKT1 were predicted by CPORT (Consensus Prediction Of interface Residues in Transient complexes) webserver (de Vries and Bonvin, 2011) and were intergraded in haddock program. Haddock server predicted most probable protein protein interaction interfaces (PPI) between NMP27: AKT1 and MP27: AKT1. The best complexes were selected with the least Haddock score. Additionally, the distance between the AKT (ATP binding pocket GKGTFG) and

phosphorylation sites within MP27 and NMP27 were determined by pymol (v1.3). Further Delphi (Li *et al*., 2012) was used for calculating electrostatic charges on the surface of NMP27, MP27, NMP27 AKT: and MP27: AKT protein complexes.

Chapter 4

RESULTS

Optimum healing of cutaneous wound requires well synchronized complex molecular events of inflammation, new tissue formation and remodeling (Singer and Clark, 1999). Stem cells in the basal layer undergo continuous proliferation and differentiation into mature keratinocytes. They maintain homeostasis of epidermis throughout life and form the new epidermis after injury. Several growth factors such as EGF, HB-GF and TGF- α are considered to regulate keratinocyte proliferation by activating EGFR downstream signaling (Martin, 1997). Thus, suggesting a key role of EGFR during re-epithelization phase (Wenczak *et al.*, 1992). Recent studies have found LRIG1 as the potent inducible feedback inhibitor of EGFR in epithelial cancer. In addition, role of LRIG1 in maintaining homeostasis within intestinal stem cell compartments has been explored. Moreover, mice deficient in LRIG-1 gene exhibited histopahological features similar to psoriatic skin. However, whether LRIG1 regulates EGFR in normal physiological process such as wound healing is not yet known. Several cell populations in sebaceous glands and hair follicles express different cell lineage markers including leucine-rich repeat-containing G-protein coupled receptor 5 (Lgr5), keratin 15 (K15) and Lrig1(Jaks *et al.*, 2010). Stem cells expressing these markers remain in quiescent state with highly potent proliferation potential during stress situation such as wound healing. Recently, it was found that $K15^{+}$ and Lgr5+ progeny of stem cells in the hair follicle contribute to wound repair (Ito *et al.*, 2005;

Jaks *et al.*, 2010). In consistent with these findings mice deficient in hair follicles on their tails showed delayed re-epitheliazation post incisional wounding (Langton *et al.*, 2007). Therefore whether stem cells expressing Lrig1 also contribute in wound repair is a question which needs to be addressed.

The aim of this study was to determine the expression of Lrig1 in different cell populations in the skin and to determine any variation in the expression of Lrig1 during normal physiological processes such as wound repair and regeneration. Further, it would to interesting to find the sub-cellular localization of Lrig1 which will enhance the understanding of its function.

4.1 EXCISIONAL WOUNDING

The mice excisional wound healing models have been widely used to study wound healing, cutaneous regeneration, stem cell and tissue transplantation and immune rejection (Wang *et al.*, 2013a). In the current study, excisional wound healing model was applicable because we aimed to determine the protein expression of LRIG1 gene during each phases of wound healing. A total of 20 Female Balb/c mice (8-16 weeks old, weighing 30-45gm) were given 5mm excisional wounds in two independent studies. Digital images were taken at different time points as mentioned earlier. It is important to take wound images and to measure the area of the wound in order to know that wounds healed under normal conditions. Time defined for wound healing may vary on environmental conditions and genetic basis of animals. Thus the

wound healing was regularly monitored by taking digital images and measuring the wound area with the help of a vernier caliper.

4.1.1 Progress of wound healing on different of wound healing

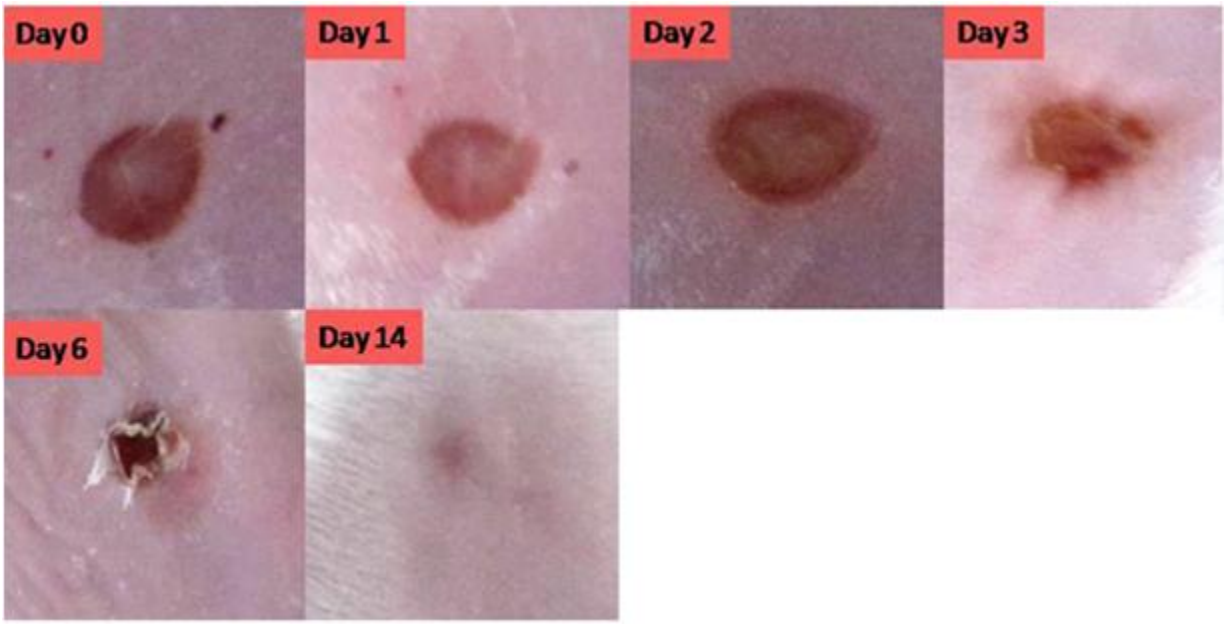

Figure 4.1: Representative macroscopic views of skin wounds in mice on time points: 0, 1, 2, 3, 6 and 14 days post wounding. This wound healing was monitored by taking digital photographs.

Digital images of wounds showed that wound healed within 14 days post wounding. From day 1-2 the wound the regions neighbouring wounds seemed swelled. On the 3rd day wound seems to contract. On the 6th day a scab (eschar) is present which is normally formed during healing process. On the 14th day a wound seemed to be healed completely however a scar was present which might take days to resolve.

4.1.2 Percentage wound contraction at different days of wound healing

Percentage wound contraction was measured at day points 0, 1, 2, 3, 6 and 12 as shown in the figure 4.2. Mice were sacrificed on day 14 however, wounds completely healed at day 12. Area was calculated for every wound through calculating length and width by vernier caliper. Later the percentage wound contraction was measured according to the formula adapted by nature's protocol (Wang *et al.*, 2013)

Area of original wound (Lx W) − area of actual wound (Lx W) /area of original wound × 100

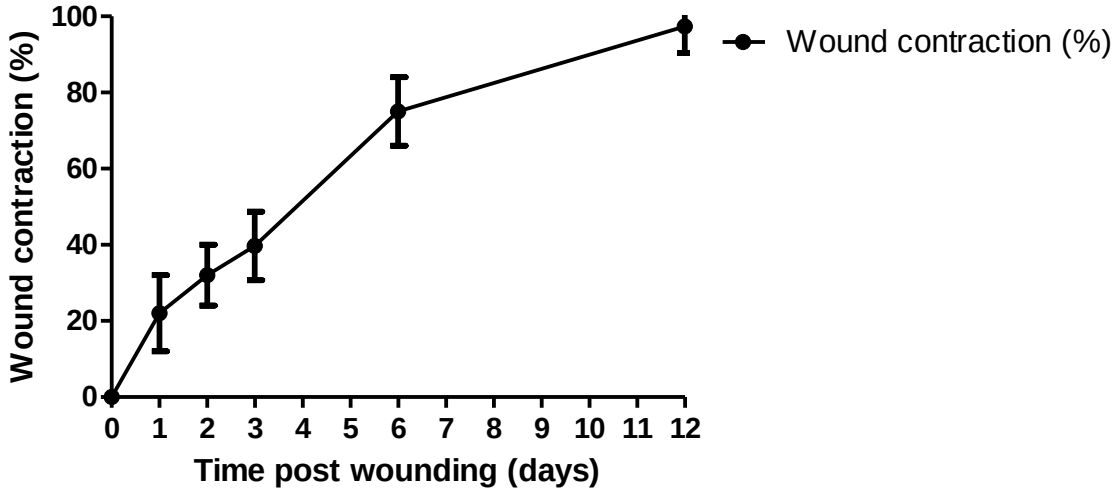

Figure 4.2: Graphical representation of percentage wound contraction. Wounded area was measured by varnier caliper. A total of four animals with six wounds (n=6) were assessed in two independent experiments on each day (Vertical lines represent standard deviation)

Percentage wound contraction graph depicts that the wound healed smoothly, where wound contraction 80% from day 0 to 6 and is just 20% from 6 to 14 days post wounding.

4.2 HEMATOXYLIN AND EOSIN STAINING

Hematoxylin and eosin (H&E) are well known for their diagnostic purposes for over a century. They are essential in recognizing the morphology of different cell and tissues. Where hematoxylin has a deep blue - purple color and stains the nucleus. In addition eosin stains proteins and in well fixed tissues it stains the cytoplasm with pink stains (Fischer *et al.*, 2008). In this study, skin tissue sections on different days were H&E stained to see different morphological change which arises after wounding as shown in figure 4.3.

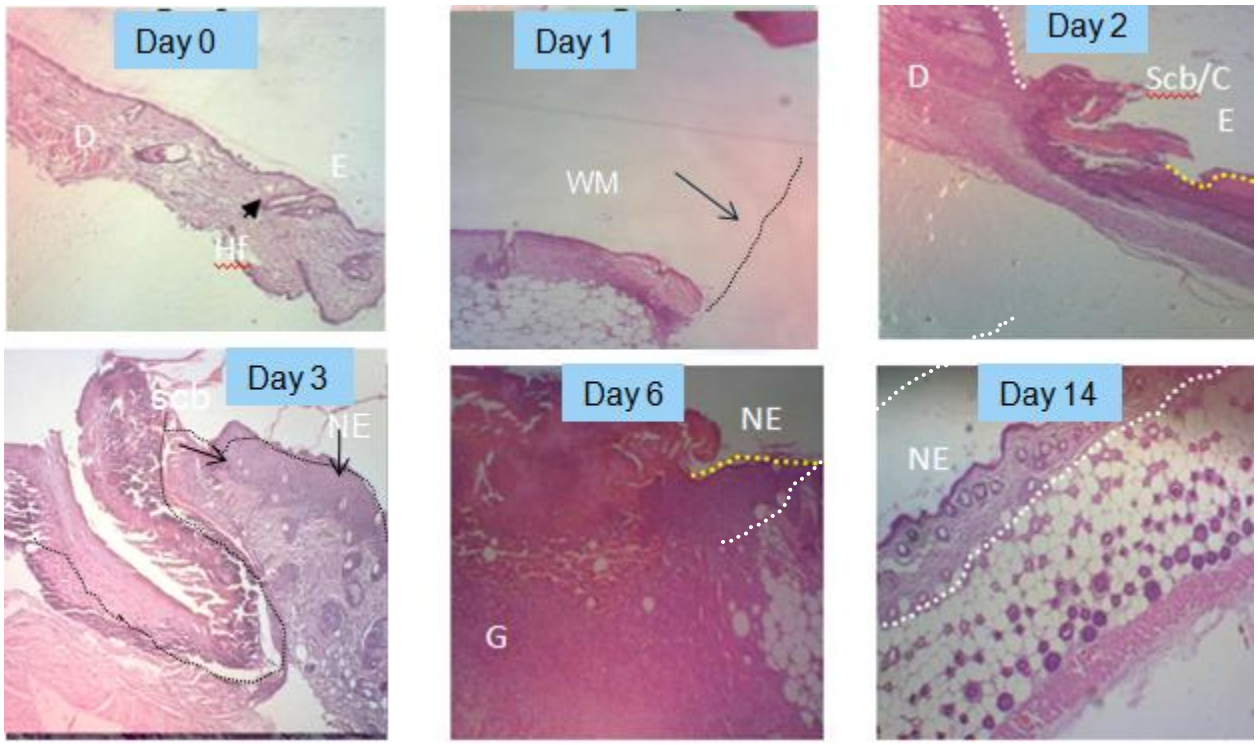

Figure 4.3: A Representative 40X images display H&E stained proximal and distal region of the wound section of 0,1,2,3,6,14 days. Abbreviation indicate E: epidermis, D: dermis, NE: new epidermis, G: granulation tissue, Scb: scab, Sb: sebaceous gland, Hf: hair follicles

At day 0 H&E stained slides show different layers of the skin, the top most layer is the epidermis which acts as a barrier and protects the skin from any chemical and infectious agents. Below the epidermis is dermis which is rich in blood vessels and glands. On day 1 the wound margins can be seen with blood clot between the wound margins. On day 2, a scab also known as eschar starts to form with a granulation tissue exactly underneath it. At day 3 and 6 eschar is present and eschar withers between day 4 to 7; the size of the granulation tissue increases and new epidermis starts to form,

bridging the wound margins. At day 14 the wound has completely healed however, the new epidermis is thick and with excessive new appendages.

4.3 IMMUNOHISTOCHEMICAL ANALYSIS OF LRIG1 PROTEIN EXPRESSION

Immunohistochemistry is an approach that helps in the detection of proteins in the tissue samples with the help of immune interactions i.e. antigen-antibody interactions in the tissue sections. It is an important tool for biological research tool in order to analyze the protein expression in tissues. In our study, the tissue sections taken on different days were stained with anti-LRIG1 antibody. The expression of LRIG1 was determined in epidermis, new epidermis, dermis and different appendages. The sections were counterstained with hematoxylin to stain the nucleus. The images of IHC stained sections in different tissues are shown in figure 4.4a & b

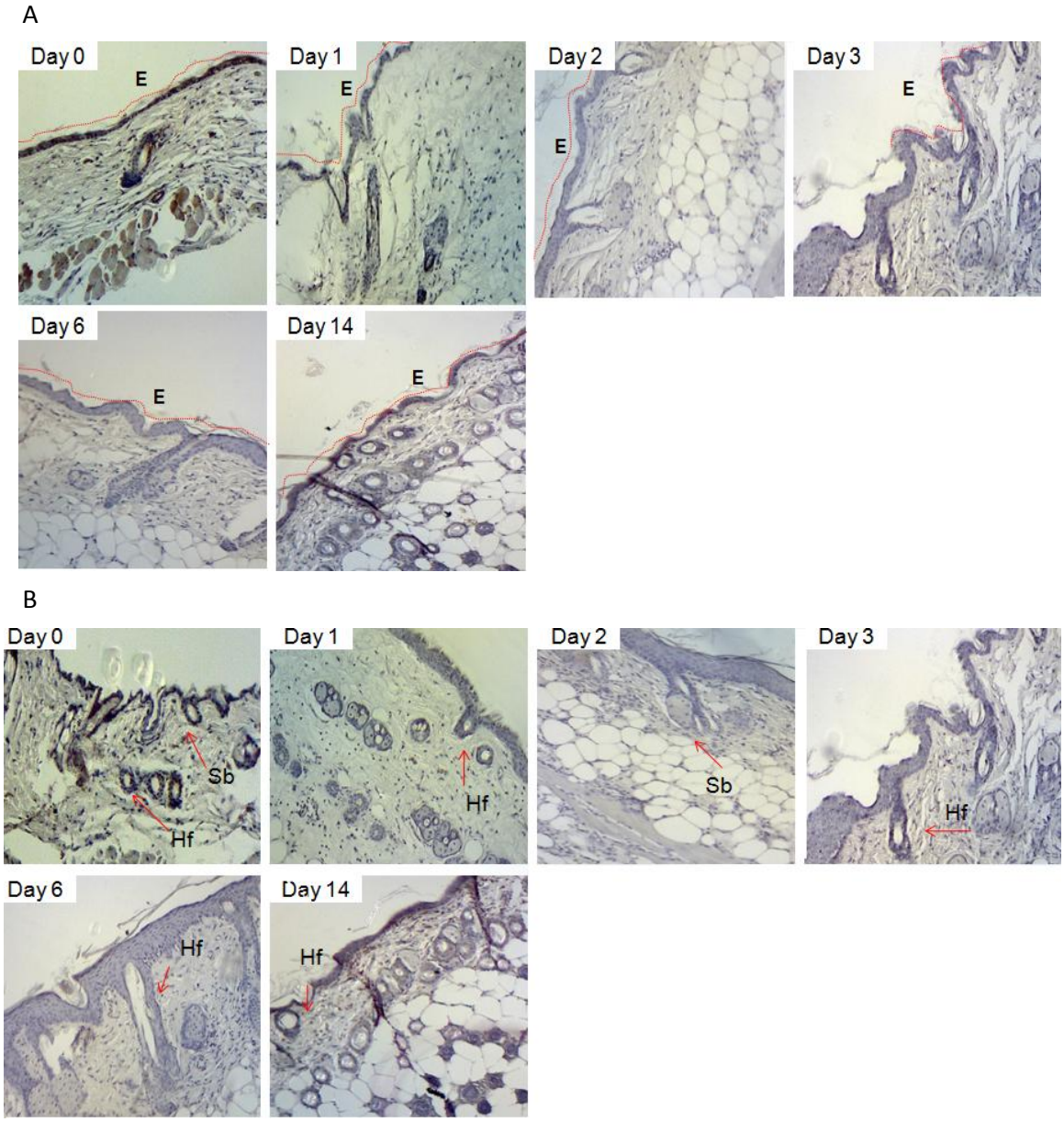

Figure 4.4a: Representative 100X images display proximal and distal region of the wound section of 0,1,2,3,6,14 days. A. LRIG1 expression in epidermis. B. LRIG1 expression in appendages (hair follicles and sebaceous gland). Sections were stained with anti- LRIG1 antibody (shown by brown region). Hematoxylin stained nuclei (shown by blue colour). Arrows and abbreviation indicate E: epidermis, Hf: hair follicles. N= 6 slides were analyzed per day.

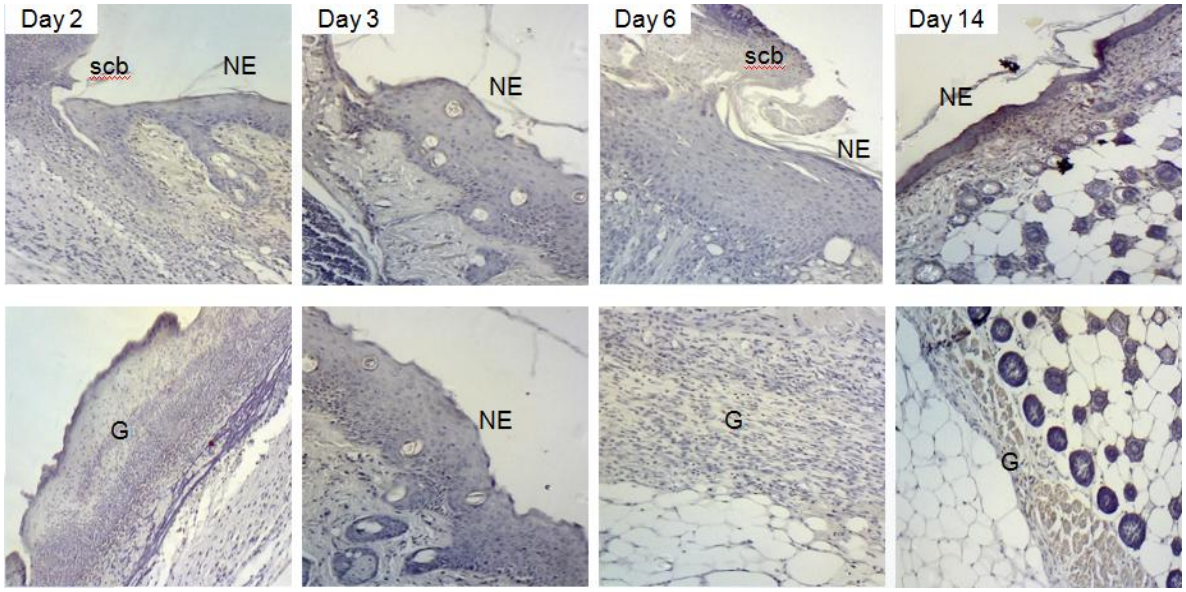

Figure 4.4b: Representative 100X images display LRIG1 expression in granulation tissues and neo epidermis at day 2, 3, 6, 14 days. Sections were stained with anti-LRIG1 antibody (shown by brown region). Hematoxylin stained nuclei (shown by blue colour). Arrows and abbreviation indicate dermis, NE: neo epidermis, G: granulation tissue, Scb: scab. N= 6 slides were analyzed per day.

4.4 PROGRESS OF LRIG1 EXPRESSION AT DIFFERENT DAYS OF WOUND HEALING

At day 0 the expression of LRIG1 was highest and least at day 6 in comparison with other days in epidermis, dermis and appendages. The expression started to gradually decline at day 1 post wound and became least at day 6. Expression was found to increase at day 14 post wounding where wound is completely healed. In addition there was no LRIG1expression in neo-epidermis, epidermis and granulation tissue at day 2, 3 and 6. The

intensity of LRIG1 was scored as 4 for highest intensity which was at day 0 and least intensity at day 6 as 1 and a graph was plotted, shown in figure 4.5 to depict the LRIG1 expression qualitatively.

A

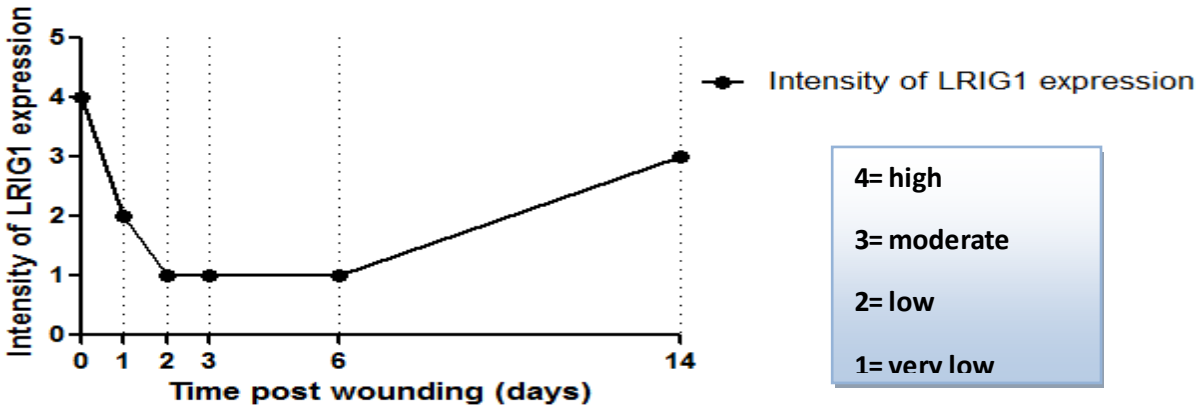

B

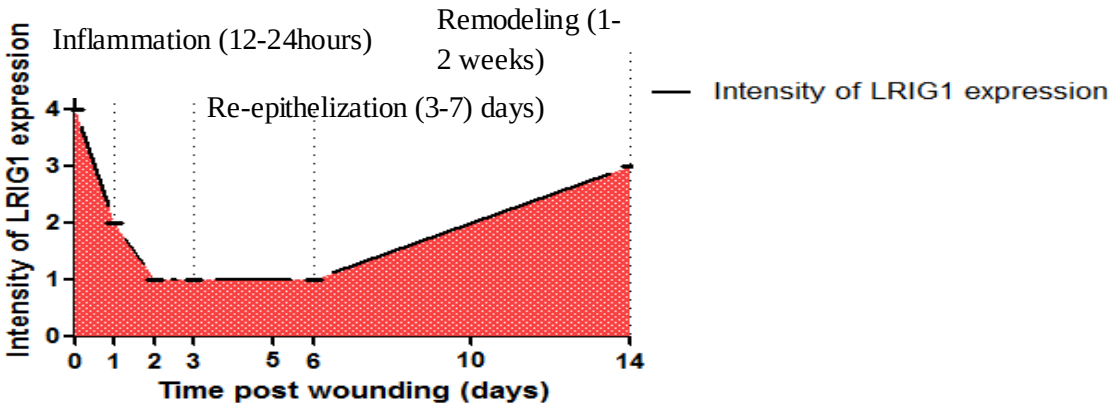

Figure 4.5: A. Intensity of LRIG1 expression on different days of wound healing. B The expression of LRIG1 was highest on day 0 (pre wounding), however the expression decreased during the inflammatory phase which lasts for first 24 hours post wounding. In addition, it was observed to remain at very low level during the re-epithelization phase in

day 2, 3 and 6. Interestingly, the expression was found to increase during the remodeling phase at day 14.

4.5 SEQUENCING AND MUTATIONAL ANALYSIS

Our sequence was aligned with a wild type consensus sequence derived from existing sequence in NCBI mentioned in section 3.7. An insertion of 3 nucleotides GTT was found at position 4-6 nucleotides (c.4_6insGTT according to Den and Antonarakis, 2000) which lead to a protein variant having an additional valine a hydrophobic residue at second position of p27 protein. Moreover, there was no change in secondary structure elements at this site of mutations. Moreover, a deletion of a single nucleotide Adenine was found at 520^{th} position (c.520delA)**,** which implicated a frame shift mutation at C terminus and resulted in alteration of entire reading frame. In addition an AKT1 phosphorylation site RKRPAT (R: Arginine, L: Lysine, P: Proline A: Alanine, T: Threonine) (Shin *et al.*, 2002) present within its nuclear localization sequence (NLS; amino acids 151–166) remained un altered. In addition, B hairpins (61-71), B strand (75-81) and helix (residues 85-90) which interact with Cdk2 and the LFG motif which bind with cyclin A (Alicia A *et al.*, 1996) all remained unchanged. Wild type amino acid residues following from 174^{th}position which were NVSDGSPNAGSVEQTPKKPGLRRRQT were replaced by MFQTVPQMPVLWSRRPRSLASEDVKR amino acid residues (figure 4.6). Interestingly, this mutated region was found to be conserved in all p27 orthologs other then mouse and chicken (figure 4.8).

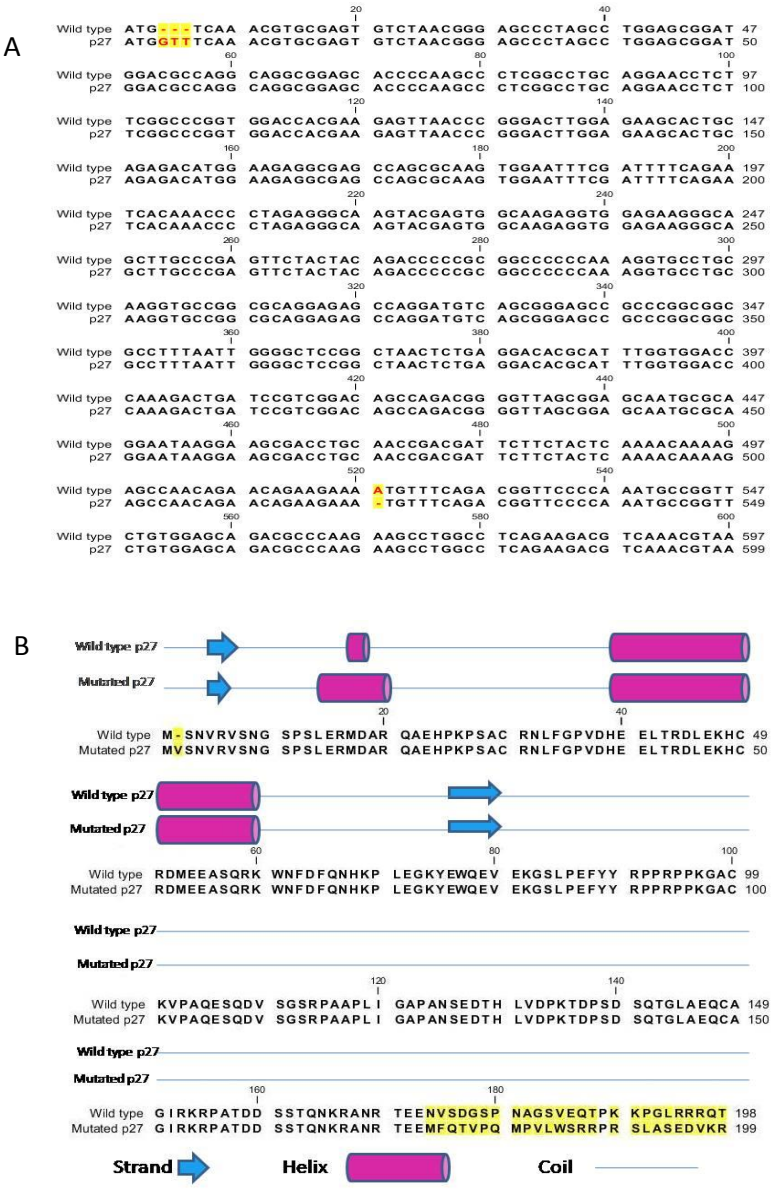

Figure 4.6: Sequence alignments of wild type and mutated p27. (A) Nucleotide sequence alignment of the wild type (NMP27) and mutated p27 (MP27). Colored residues indicating insertion and deletion in MP27 (B) Protein sequence alignment of wild type (NMP27) and mutated p27 (MP27). Uncoloured residues are identical in both. Mutated residues are highlighted with yellow colour. Predicted secondary

structure elements for wild type p27 and mutated p27 shown by strands, helix and coils.

4.6 MODELING

Protein sequence of CDKN1B which was submitted in (PSI)-BLAST facility showed 80% sequence identity with P27 (PDB codes: 1JSU). However, this structure lacked complete query coverage and our interest areas: N and C terminus. Webservers Quark and Robetta generated fifteen 3D models for complete P27 protein. Model 4 generated from Robetta was rated as the best model on the basis of ERRAT, Rampage and QMEAM scores. PROCHECK-based Ramachandran map statistics found 87.8 % of Model 4 amino acid residues in the favored region, 11% in the additionally allowed region and only 0.6 % residues in the disallowed region. These results indicate that this model has protein structure with favorable sterio-chemical property (Laskowski *et al.*, 1993). Moreover, Z score was found to be -2.97 and Qmean score of 0.488. After refinement of predicted residues present in disallowed regions, the overall quality factor of the abnitio model was 90.86 % in the ERRAT plot and it showed few atomic attractions creating steric hindrance between amino acids (figure 4.7).

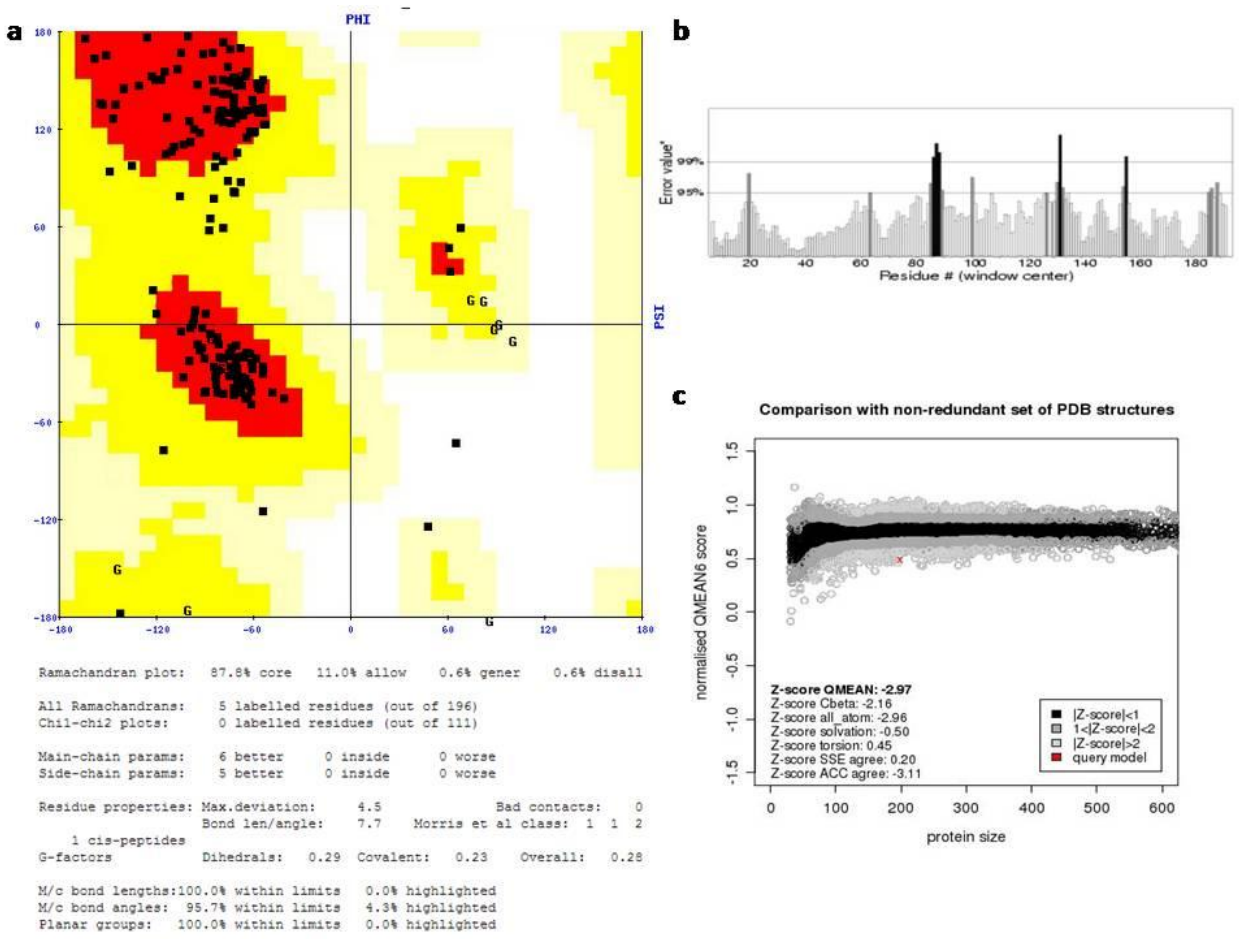

Figure 4.7: Evaluation of model 4. a PROCHECK based Ramachandran map, b ERRAT plot , c Q-mean Z-score plot

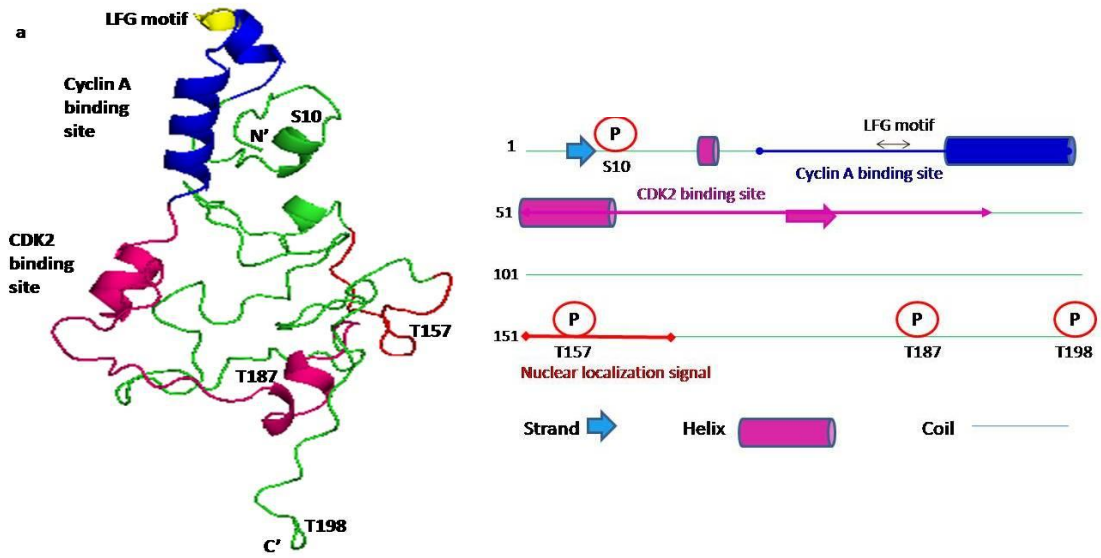

b

	160			180			
P27 Human	IRKRPATDDS	STQNKRANRT	EENVSDGSPN	AGSVEQTPKK	PGLRRRQT	198
P27 Chimpanzee	IRKRPATDDS	STQNKRANRT	EENVSDGSPN	AGSVEQTPKK	PGLRRRQT	198
P27 Cat	IRKRPATDDS	SPQNKRANRT	EENVSDGSPN	AGSVEQTPKK	PGLRRRQT	198
P27 Dog	IRKRPATDDS	SPQNKRANRT	EENVSDGSPN	AGSVEQTPKK	PGLRRRQT	198
P27 Mouse	MRKRPAAEDS	SSQNKRANRT	EENVSDGSPN	AGTVEQTPKK	PGLRR-QT	197
P27 Chicken	QRKRPAADDS	SPQNKRANTT	EEEVSEDSPS	ASSVEQTPKK	SSPRRHQT	198
Consensus	IRKRPATDDS	SPQNKRANRT	EENVSDGSPN	AGSVEQTPKK	PGLRRRQT	

Figure 4.8: a. Ribbon and a linear representation of p27 protein. C,N showing terminal ends of protein, Ser10, T157, T187 and T198 are key phosphorylation sites in p27, Cyclin A binding domain (blue), LFG motif (yellow) , CDK2 binding site (pink), Nuclear Localization signal (red). The ribbon figure was produced using Pymol (v1.3). b Highly conserved consenses sequence of C terminal end of p27 orthologs.

4.7 PROTEIN-PROTEIN INTERACTIONS

P27 was docked with AKT1 via Haddock web server, 145 water refined complexes were generated, grouped in 10 clusters. The Haddock score, buried surface area, Z score, RMSD, Electrostatic energy, Cluster size, van der waals energy, desolvation energy, restrains violation energy for all the clusters are shown in figure 4.9**.** A complex of p27 and AKT1 with a haddock score of -71.5± 10.2 was selected as the best probable complex. Further, Haddock predicted 147 water refined complexes for MP27 and AKT1. Cluster 2 was rated as the best complex with a Haddock score of -138.4± 10.1 and the rest of the criterion generated by haddock are shown in figure 4.10. Additionally, the distance between the AKT (ATP binding pocket GKGTFG) and phosphorylation sites within MP27 and NMP27 were determined by pymol (v1.3). Interestingly the distance for S10 phosphorylation site for mutated p27 decreased, however the distance between T157 and ATP binding pocket increased.

Further, electrostatic potential maps were used to illustrate charge distribution on the surface of AKT1 (figure 4.13), NMP27, MP27 and their complexes. In non mutated model (NMP27), negative (depicted by red colour) and positive charges (blue colour) were uniformly distributed at its C terminal (figure 4.12). However, in MP27 the positively charged surfaces were more in comparison with negative charges at its mutated C terminal.

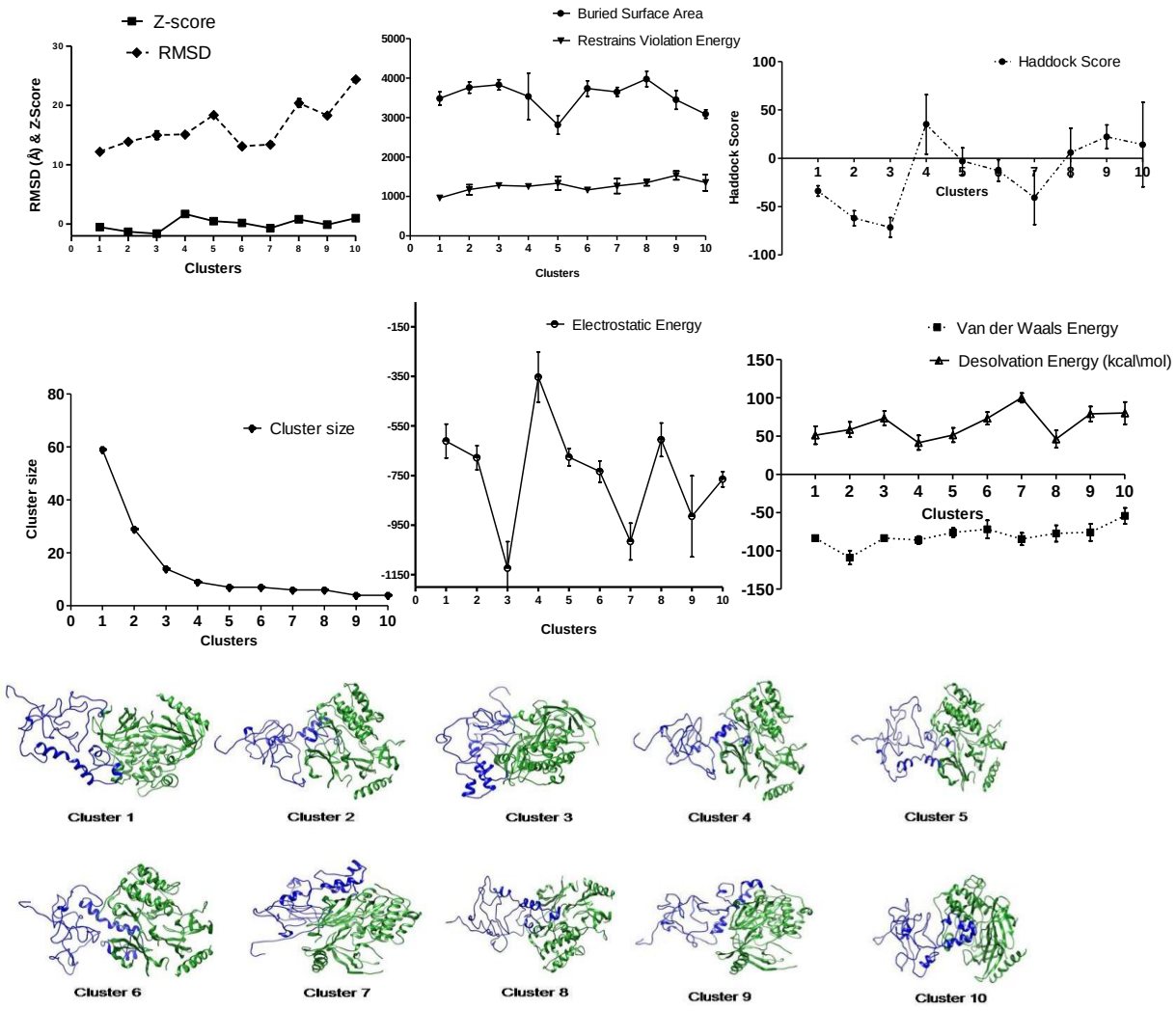

Figure 4.9: Graphical representation of scores generated by Haddock for clusters 1-10. B: Superposed Cartoon AKT: P27 complexes 1-10 generated by Haddock, P27 highlighted in blue and AKT1 in green colour.

Haddock scores of PPI (MP27: AKT1)

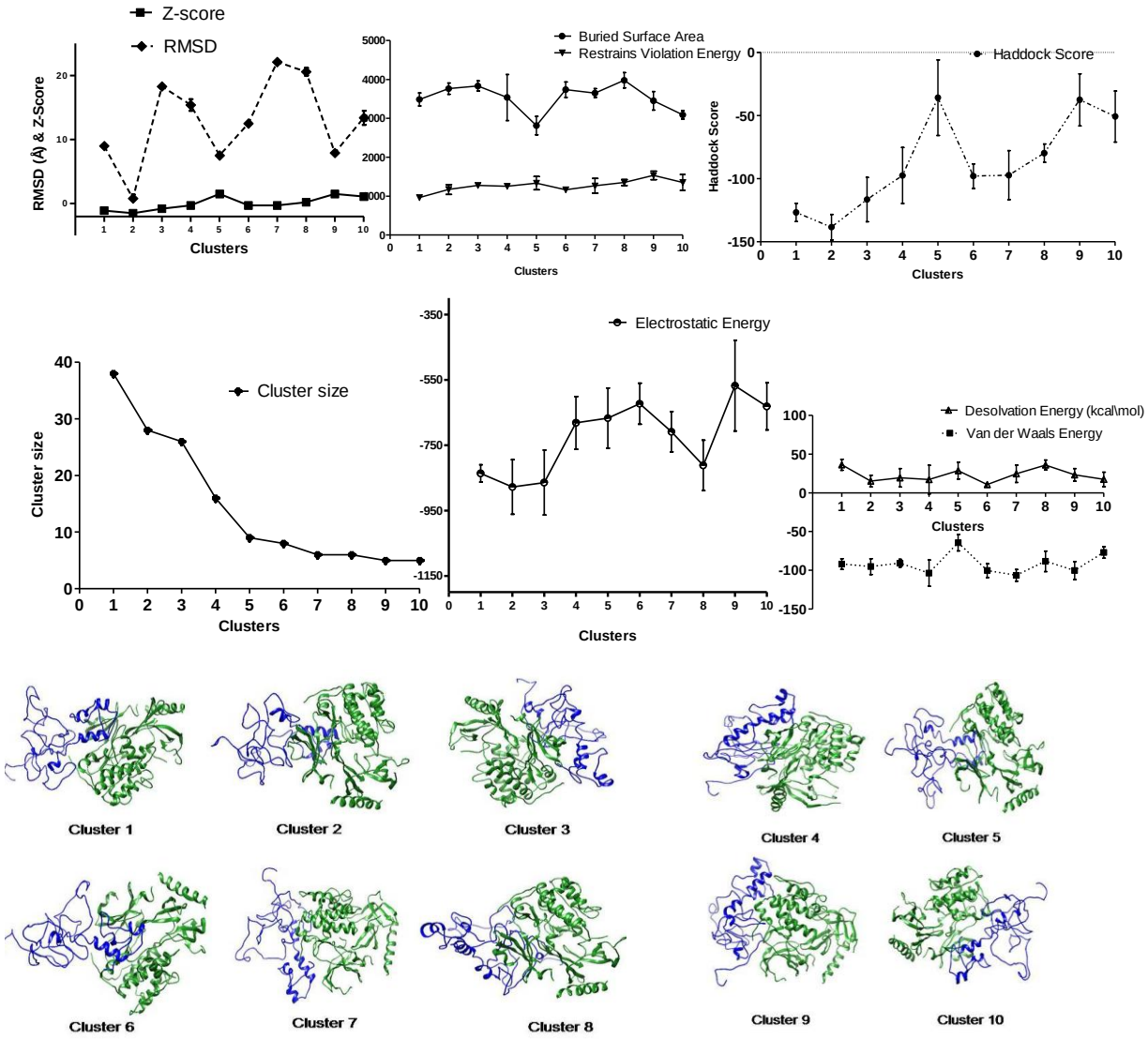

Figure 4.10: Haddock generated scores of protein- protein interaction (PPI) between mutated p27 and AKT1. B: Cartoon representation of complexes 1-10 (MP27: AKT1) generated by Haddock, mutated P27 highlighted in blue and AKT1 in green colour.

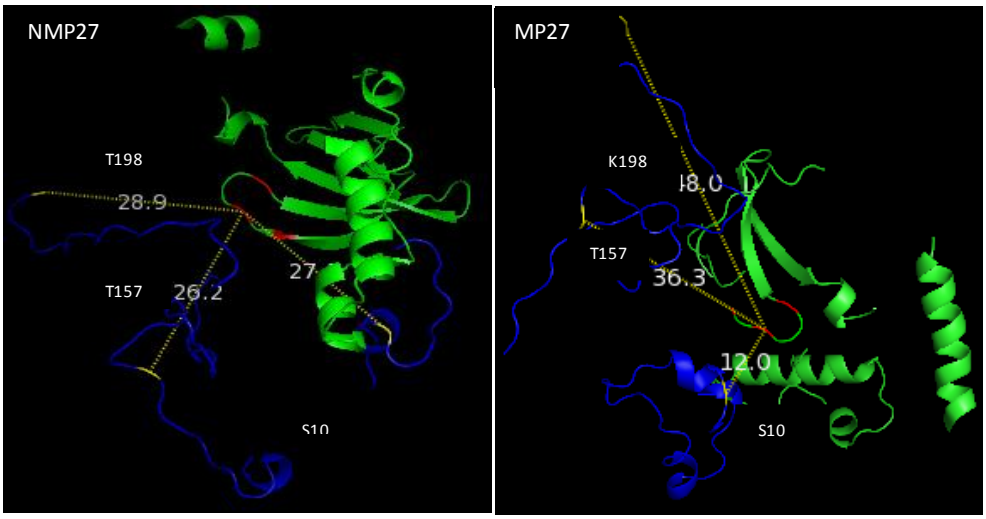

Figure 4.11: Ribbon presentation of distance between AKT (ATP binding pocket) and AKT phosphorylation sites T198, T157, S10 as for NMP27 and K198, T157, S10 for MP27. The figure was produced using Pymol (v1.3).

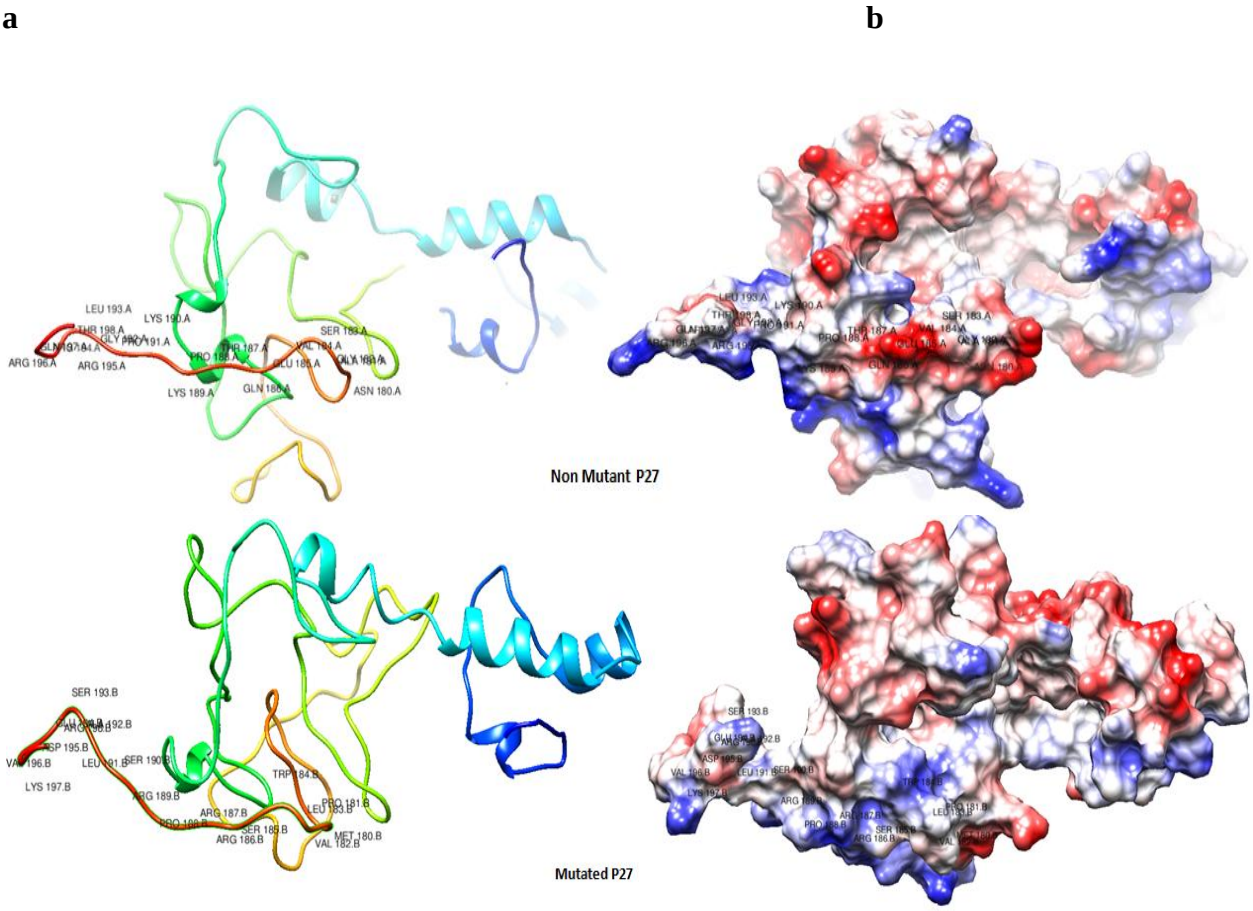

Figure 4.12: Cartoon representation of non mutated and mutated p27 with comparison of electrostatic potentials (a) Altered amino acids at C terminal are shown in Non mutated and mutated p27 models. (b) Comparison of the electrostatic potential on the surface of residues for both structures. It is demonstrated that in non-mutated p27 model the C terminal region is somewhat mixture of negatively and positively charged residues, whereas in mutant model the coulombic surface is showing a trend of positively charged regions (blue positive charges, red negative charges).

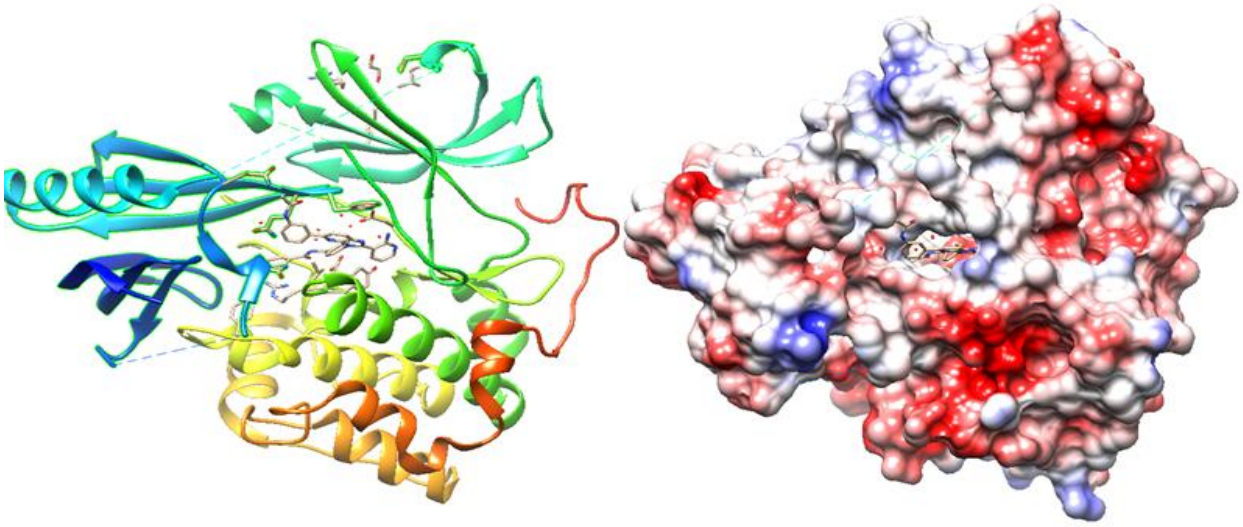

Figure 4.13: (a) Human AKT in complex with an alloesteric inhibitor (PDB ID no. 3O96). An alloesteric inhibitor (shown in sticks) binds with human AKT into the deep ATP-binding cleft. (b) Electrostatic potential map of this complex (The protein surface is colored based on the electrostatics (blue positive charges, red negative charges).

4.7 SUPPLEMENTARY DATA

Table 4.8: Supplementary data (Area in millimeter/percentage of wound contraction %)

	A/WC1	A/WC2	A/WC3	A/WC6	A/WC12
W1	14.13/32.6	19.9/5.1	8.34/31.8	2.4/88.54	0.28/98.4
W2	13.64/-1.19	19.3/-43.2	12.21/32	3.05/77.4	0.63/96.4
W3	11.4/-4.06	7.56/31	10.12/-18.7	4.32/86.3	0.81/95.1
W4	17.8/-47	11.48/5.1	16.2/16.1	3.31/89.6	0.81/94.6
W5	14.3/7.98	17.86/-14.9	6.22/66.7	2.55/75	
W6	44.3/-78	9.5/32.3	30.47/10.16	4.32/72.2	
W7	14.92/25.8	12.76/36.5	10.1/61.5	75/12	
W8	34.1/0.93	34.2/0.64	8.95/65	4.65/62	
W9	18.9/-30.9	14.006/55.7	7.65/45.5	1.87/89.6	
W10	19.92/-71	21.465/32.7	9.8/32.4	1.8/93	
W11	18.9/40.2	13.152/-12	9.14/30.2	2.55/90	
W12	26.5/16.9	15.04/7.6	17.88/14.7	2.38/83	
W13	14.097/36.9	10.14/60.7	12.9/4.3	3.78/74	
W14	16.43/-5.8	18.31/22.9	6.332/47.7		
W15	17.63/-34.7	8.4/57.3	16.28/-4.76		
W16	20.24/14.8	11.48/56.3	9.75/51.5		
W17	14.82/25.3	32/20	26.38/23.4		
W18	22/18	9.99/18.4	6.84/78.4		
W19	9.98/18.5	9.18/49	6.77/78.8		
W20	22.32/-24	5.88/70.3	6.77/34.3		
W21	11.12/43.9	16.32/-91	13.75/11.5		
W22	15.84/-86	14.52/24.8	8.4/57.7		
W23	18.1/5.95	15.08/-15.5	39.67/20		
W24	23.87/-24.4	9.84/47.3			
W25	18.65/0.054	20.21/27			
W26	26.15/5.46	13.94/-			
W27	21.12/-75.85	14.06/3			
W28	18.03/38.4				
W29	10.04/61.8				
W30	13.63/47.2				
W31	10.92/22.2				

Area(mm)/percentage wound contraction (A/WC), Wounds No (Wx)

Chapter 5

DISCUSSION

Recently, there is an emerging interest in context with LRIG1 protein due to its key role as a tumour suppressor (Wang *et al.*, 2013). LRIG1 deregulates EGFR signaling in embryonic kidney-293 cells, keratinocytes, bladder carcinoma cells, glioma cells and epithelial cancers. LRIG1 gene ablation in mice leads to psoriasis like phenotype and increased EGFR signaling in keratinocytes (Powell *et al.*, 2012) indicating an important role of LRIG-1 in the skin homeostasis, therefore we aimed to explore the LRIG-1 expression during various stages of wound healing. Moreover, in this study we determined the protein expression of LRIG1 in full thickness epidermal excisional wound healing murine model. Mice skin tissue sections were taken at day 1, 2, 3, 6 and day 14 after wounding in context to the days selected by Repertinger *et al.*, 2004. These days are important with reference to the wound healing as the early inflammatory phase takes place during the first 24 hrs and the next re-epithelialization takes place between 2-6 days, and the re-modeling phase starts after 7^{th} day (Gurtner *et al.*, 2008). As predicted, varying expression of LRIG1 was observed on different post-wounding days. The highest expression of LRIG-1 was found to be expressed at day 0 in the nucleus and cytoplasm of varying cell populations such as hair follicles, sebaceous glands and keratinocytes. There was a gradual decline in the LRIG-1 expression in the inflammatory and re-epithelialization phase from post wounding day 1 to 6 while an upregulated expression was observed on day 14. Therefore, we can infer from previous study and imply that LRIG1 expression is high at day 0 in order to

maintain quiescent state of interfollicular stem cells. Moreover, it was found that lrig1 expression was low at day 1 and very low at day 2, 3 and day 6. As mentioned earlier regeneration phase is between days 3, where there is a surge of keratinocytes to the site of the wound. EGFR is the key mediator of proliferation, migration of keratinocytes and inversely related to LRIG1 expression. On the other hand LRIG1 is expressed in stem cells to retain stem cells at non dividing state. At day 14, wound was completely healed and LRIG1 expression was present in different cell populations. However, the expression was less in comparison with day 0 but more than the rest of the days. There is a rise in the expression of LRIG1 because the stem cells revert to their quiescent phase and express LRIG1 to inhibit EGFR signaling. In earlier studies, Powell and his team reported that lrig1 marks non dividing, long-lived stem cells residing in the crypt base of small intestine in response to injury, proliferate and divide to restore the damaged crypts in small intestine. Further they showed that Lrig1 knockout mice exhibits increased number of intestinal stem cells and later develops duodenal adenomas. LRIG1 gene ablation in mice leads to psoriasis like phenotype and increased EGFR signaling in keratinocytes (Powell *et al.*, 2012). Moreover, c-Myc expression is upregulated in chronic wounds which suppresses the migration of keratinocytes and leads to excessive proliferation of stem cells (Waikel *et al.*, 2001; Watt, 2001). Intriguingly, downregulation of LRIG1 by RNA interference not only activated EGFR but also Protein kinase B (Akt) and c-Myc (Xie *et al.*, 2013). Taken together it can be said that LRIG-1 protein plays an important role in the stem cell niches. The downregulated LRIG-1 expressions during the re-epithelization phase

and then later increase in LRIG-1 expressions in the re-modeling phases indicate that an important regulatory role of LRIG-1 in epithelial proliferation. This is in line with the tumor suppressive role of LRIG-1 in various published studies. These findings demonstrate that LRIG1 has a significant role in wound resolution phase.

The epidermis is continuously renewing itself by highly regulated processes of keratinocytes proliferation, differentiation and programmed cell death. There are skin disorders such as keratoderma, epidermal naevi, viral warts, molluscum contagiosum, inflammatory conditions such as psoriasis and lichen planus characterized by deregulated keratinocyte proliferation resulting in epidermal hyperproliferation. The data presented here show that LRIG1 has a key role in mediating normal wound healing which would enable in bringing forth promising treatments for various skin disorders.

p27 kip1 is recognized as a tumor suppressor, mediator of apoptosis, key regulator of cell differentiation and controls drug resistance in solid tumors (Rodier *et al.*, 2001). Two different mechanisms have been inferred to be involved in p27 inactivation during tumour development: its nuclear export and enhanced protein degradation (Shin *et al.*, 2002). During G1–S transition, p27 is actively phosphorylated at Thr187 by cyclin E-CDK2 (Muller and Morris, 1989) Thr187-phosphorylated p27 is recognized by Skp2-containing E3 ubiquitin ligase, SCF, and its cofactor, Cdk subunit1 (Cks1) and which promote its degradation by proteasome (Carrano *et al.*, 1999). However, p27 sub cellular localization is dependent on phosphorylation of three key amino acid residues S10, T157, T198 by AKT. Mutation

at T157 impedes AKT1 induced phosphorylation and promotes its nuclear localization. In a study, a complete reversion of AKT1 induced cytoplasmic relocalization was demonstrated only in the presence of double mutation at T157A and T198A (Motti *et al.*, 2004). However, in cancer patients mutations in p27 gene rarely prevail as compare to other tumor suppressors such as p15 and p16 (Jen *et al.*, 1994).

In this study we report novel mutations found in p27 mRNA isolated from breast cancer patient. Firstly, there was an addition of GTT nucleotides at position 4-6 in the coding sequence which lead to an addition of valine a hydrophobic residue at second position of p27 protein. The concept of kozak consensus sequence GCCRCCaugG (where R = purine and "aug" is the initiation codon), with the -3R and +4G being particularly important for translation initiation. Kozak (Kozak, 1997) found +4G enhances translation initiation, but does not when it occurs in a GUN codon (coding for valine). Another study in Escherichia coli demonstrated consistent findings that valine at penultimate site (second position) reduces initiator Met cleavage in comparison with amino acids such as Ala, Cys, Gly, Pro, or Ser (Frottin *et al.*, 2006). In contrast few studies on prokaryotes and eukaryotes propose that cleavage of Met occurs with valine at this position (Civitelli, 1998; Moerschell *et al.*, 1990; Murphy *et al.*, 2002). Kozak consensus sequence is not the only criterion which initiates translation thus any outcome of this mutation cannot be predicted until further validation. In addition, a deletion of a single nucleotide Adenine was found at 520^{th} position**,** which implicated a frame shift mutation at C terminus and resulted in alteration of entire reading frame. Wild type amino acid residues following from

174thposition which were NVSDGSPNAGSVEQTPKKPGLRRRQT were replaced by MFQTVPQMPVLWSRRPRSLASEDVKR amino acid residues. This C terminal region was found conserved in all p27 orthologs other then mouse and chicken thus implying its significance in p27 functionality. These mutations have been reported for the first time. Although Norihiko et al and M. Veronica Ponce-Castaneda et al in independent studies found neither deletions nor rearrangements in p27 gene when screened in various soild tumors (Kawamata *et al.*,1995; Ponce *et al.*,1995). Besides, a hemizygous deletion in p27 was found in a B-cell non-Hodgkin's lymphoma (Morosetti *et al.*, 1995). In adult T-cell leukemia, a stop codon mutation at 76 was found (Morosetti *et al.*, 1995). In addition two point mutations were found during 36 primary breast carcinomas. One of the mutations in the breast carcinomas was a polymorphous mutation at codon 142 and the other a nonsense mutation at codon 104 (Spirin *et al.*, 1996).

Further, in this study we have used computer based tools to model non mutated and mutated p27. The reliability of the protein models were evaluated on several parameters including by ERRAT, Ramachandran, Qmean and Z score. Where, 90.86% ERRAT, -2.97 Z score with 0.488 Qmean score. The final p27 model which was selected had bond angles, lengths, dihedrals and interactions energy within the allowed range without atomic clashes. These results supported the use of this model as a template to model mutated p27, followed by protein protein interactions (PPIs) of P27 with AKT1. The predicted models of NMP27 and MP27 showed no structural difference relative to each other. Protein–protein interactions play a vital role in

various biological processes including signal transduction cell metabolism and muscle contraction (Mendelsohn and Brent, 1999). However, experimental analyses of PPIs have certain limitation such as a need to anticipate likelihood of interactions before initiating an experiment. Therefore, computational tools can blindly predict binding interfaces between proteins. In our study Haddock tool was used to predict most probable PPIs interfaces for NMP27: AKT and MP27: AKT with haddock score of -71.5± 10.2 and -138.4± 10.1. Electrostatic interactions are non-covalent interactions, which occur between electrically charged atoms having both positive and negative interactions (Kessel and Ben-Tal, 2012). It plays a key role in determining the nature and strength of the PPIs. Here electrostatic potential maps of AKT, NMP27, and MP27 were determined. AKT and NMP27 show even distribution of positive and negative charges. However MP27 demonstrated excessive positive charges at its mutated c terminal. Thus, it is most likely that MP27 binds less strongly with AKT in comparison with NMP27 due to electrostatic repulsion. Further, whether C terminal frameshift mutation had any effect on the remaining AKT phosphorylation sites: S10 and T157 were determined by measuring distance between the phosphorylation site and ATP binding pocket (GKGTFG) (Susan F, 2008). The distance of S10-AKT decreased from 27.3Å in NMP27 to 12Å in MP27. Moreover, distance of T157-AKT changed from 26.2Å to 36.3Å due to mutation. In conclusion, T198 and T187 phosporylation sites are altered which enhances nuclear import and decreases proteasome mediated degradation. Thus we predict that C terminal mutation will also

affect interaction of S10 and T157 with AKT which will increase p27 nuclear localization.

Chapter 6

REFERENCES

Abraira V.E., Satoh T., Fekete D.M., Goodrich L.V. (2010). Vertebrate Lrig3-ErbB interactions occur in vitro but are unlikely to play a role in Lrig3-dependent inner ear morphogenesis., PloS one, 5:e8981.

Arwert, E. N., Hoste, E., & Watt, F. M. (2012). Epithelial stem cells, wound healing and cancer., Nature Reviews Cancer, 12(3): 170-180.

Ashcroft, G. S., Horan, M. A., & Ferguson, M. W. (1997). The effects of ageing on wound healing: immunolocalisation of growth factors and their receptors in a murine incisional model., Journal of anatomy, 190(3): 351-365.

Bazley L., Gullick W. (2005). The epidermal growth factor receptor family., Endocrine-related cancer, 12:S17-S27.

Beckmann M., Niederacher D., Massenkeil G., Tutschek B., Beckmann A., Schenko G., Schnผrch H.-G., Bender H.G. (1996). Expression analyses of epidermal growth factor receptor and HER-2/neu: no advantage of prediction of recurrence or survival in breast cancer patients., Oncology, 53:441-447.

Benkert, P., Tosatto, S. C., & Schomburg, D. (2008). QMEAN: A comprehensive scoring function for model quality assessment., Proteins: Structure, Function, and Bioinformatics, 71(1): 261-277.

Ben-Levy R., Paterson H.F., Marshall C., Yarden Y. (1994). A single autophosphorylation site confers oncogenicity to the Neu/ErbB-2 receptor and enables coupling to the MAP kinase pathway., The EMBO journal, 13:3302.

Blanpain C., Fuchs E. (2009). Epidermal homeostasis: a balancing act of stem cells in the skin., Nature reviews Molecular cell biology, 10:207-217.

Borriello, A., Cucciolla, V., Oliva, A., Zappia, V., & Della Ragione, F. (2007). p27Kip1 metabolism: a fascinating labyrinth., Cell Cycle, 6(9); 1053-1061.

Boehm M , Yoshimoto T, Crook MF, Nallamshetty S, True A, Nabel GJ, Nabel EG. (2002). A growth factor-dependent nuclear kinase phosphorylates p27(Kip1) and regulates cell cycle progression., EMBO J, 21(13):3390-401.

Brem H., Tomic-Canic M. (2007). Cellular and molecular basis of wound healing in diabetes., The Journal of clinical investigation, 117:1219-1222.

Brigham, P. A., & McLoughlin, E. (1996). Burn incidence and medical care use in the United States: estimates, trends, and data sources., Journal of Burn Care & Research., 17(2): 95-107.

Bucci B., D'Agnano I., Botti C., Mottolese M., Carico E., Zupi G., Vecchione A. (1996). EGF-R expression in ductal breast cancer: proliferation and prognostic implications., Anticancer research, 17:769-774.

Cabodi S., Moro L., Bergatto E., BoeriErba E., DiStefano P., Turco E., Tarone G., Defilippi P. (2004). Integrin regulation of epidermal growth factor (EGF) receptor and of EGF-dependent responses., Biochemical Society Transactions, 32:438-442.

Cai M., Han L., Chen R., Ye F., Wang B., Han F., Lei T., Guo D. (2009). Inhibition of LRIG3 gene expression via RNA interference modulates the proliferation, cell cycle, cell apoptosis, adhesion and invasion of glioblastoma cell (GL15)., Cancer letters, 278:104-112.

Carpenter G., King L., Cohen S. (1978). Epidermal growth factor stimulates phosphorylation in membrane preparations in vitro.

Carrano, A. C., Eytan, E., Hershko, A., & Pagano, M. (1999). SKP2 is required for ubiquitin-mediated degradation of the CDK inhibitor p27., Nature cell biology, 1(4); 193-199.

Chamian F., Krueger J.G. (2004). Psoriasis vulgaris: an interplay of T lymphocytes, dendritic cells, and inflammatory cytokines in pathogenesis., Current opinion in Rheumatology, 16:331-337.

Chen J., Jackson P.K., Kirschner M.W., Dutta A. (1995). Separate domains of p21 involved in the inhibition of Cdk kinase and PCNA.

Chu I.M., Hengst L., Slingerland J.M. (2008). The Cdk inhibitor p27 in human cancer: prognostic potential and relevance to anticancer therapy., Nature Reviews Cancer, 8:253-267.

Civitelli, G. (1998). The Meso-cenozoic sedimentary sequence of the Cabo-Delgado province, Mozambique., Journal of African Earth Sciences and the Middle East, 6(9): 9-12.

Clark, R. (1996). The molecular and cellular biology of wound repair: 2nd ed. New York: Plenum Press

Clark, R. A. (1990). Fibronectin matrix deposition and fibronectin receptor expression in healing and normal skin., Journal of Investigative Dermatology, 94: 128s-134s.

Cohen S. (1997). EGF and its receptor: historical perspective., Journal of mammary gland biology and neoplasia, 2:93-96.

Crew F.A. (1933). Waved: an autosomal recessive coat form character in the mouse., Journal of Genetics, 27:95-96.

de Vries, S. J., & Bonvin, A. M. (2011). CPORT: a consensus interface predictor and its performance in prediction-driven docking with HADDOCK., PLoS One, 6(3): e17695.

De Vries, S. J., van Dijk, M., & Bonvin, A. M. (2010). The HADDOCK web server for data-driven biomolecular docking., Nature protocols, 5(5): 883-897.

Den D. J.T and Antonarakis S.E., (2000). Hum. Mutat. 15:7-12

Eccles S.A. (2011). The epidermal growth factor receptor/Erb-B/HER family in normal and malignant breast biology., International Journal of Developmental Biology, 55:685.

Eswar, N., Webb, B., Martin, Renom, M. A., Madhusudhan, M., Eramian, D., Shen, M. y., Sali, A. (2006). Comparative protein structure modeling using Modeller., Current protocols in bioinformatics, 5.6: 1-5.

Falls D.L. (2003). Neuregulins: functions, forms, and signaling strategies., Experimental cell research, 284:14-30.

Ferguson K.M., Berger M.B., Mendrola J.M., Cho H.-S., Leahy D.J., Lemmon M.A. (2003). EGF activates its receptor by removing interactions that autoinhibit ectodomain dimerization., Molecular cell, 11:507-517.

Fero, M. L., Rivkin, M., Tasch, M., Porter, P., Carow, C. E., Firpo, E., Perlmutter, R. M. (1996). A Syndrome of Multiorgan Hyperplasia with Features of Gigantism, Tumorigenesis, and Female Sterility in p27< i> Kip1</i>-Deficient Mice., Cell, 85(5): 733-744.

Fiorentino L., Pertica C., Fiorini M., Talora C., Crescenzi M., Castellani L., Alem S., Benedetti P., Segatto O. (2000). Inhibition of ErbB-2 mitogenic and transforming activity by RALT, a mitogen-induced signal transducer which binds to the ErbB-2 kinase domain., Molecular and cellular biology, 20:7735-7750.

Fischer A.H., Jacobson K.A., Rose J., Zeller R. (2008). Hematoxylin and eosin staining of tissue and cell sections., Cold Spring Harbor Protocols 2008, pdb. prot4986.

Fischer-Colbrie J., Witt A., Heinzl H., Speiser P., Czerwenka K., Sevelda P., Zeillinger R. (1996). EGFR and steroid receptors in ovarian carcinoma: comparison with prognostic parameters and outcome of patients., Anticancer research, 17:613-619.

Frottin, F., Martinez, A., Peynot, P., Mitra, S., Holz, R. C., Giglione, C., & Meinnel, T. (2006). The proteomics of N-terminal methionine cleavage., Molecular & Cellular Proteomics, 5(12); 2336-2349.

Garrett T.P., McKern N.M., Lou M., Elleman T.C., Adams T.E., Lovrecz G.O., Zhu H.-J., Walker F., Frenkel M.J., Hoyne P.A. (2002). Crystal structure of a truncated epidermal growth factor receptor extracellular domain bound to transforming growth factor., Cell, 110:763-773.

Gottrup, F., Apelqvist, J., & Price, P. (2010). Outcomes in controlled and comparative studies on non-healing wounds: recommendations to improve the quality of evidence in wound management., Journal of wound care, 19(6): 237-268.

Greiling, D., & Clark, R. (1997). Fibronectin provides a conduit for fibroblast transmigration from collagenous stroma into fibrin clot provisional matrix., Journal of cell science;,110(7): 861-870.

Grose R., Werner S. (2004). Wound-healing studies in transgenic and knockout mice., Molecular biotechnology, 28:147-166.

Gur G., Rubin C., Katz M., Amit I., Citri A., Nilsson J., Amariglio N., Henriksson R., Rechavi G., Hedman H. (2004). LRIG1 restricts growth factor signaling by enhancing receptor ubiquitylation and degradation., The EMBO journal, 23:3270-3281.

Gurtner G.C., Werner S., Barrandon Y., Longaker M.T. (2008). Wound repair and regeneration., Nature, 453:314-321.

Heldin, C.-H., & Westermark, B. (1988). Role of platelet-derived growth factor in vivo The molecular and cellular biology of wound repair (pp. 249-273): Springer.

Henseler T., Christophers E. (1985). Psoriasis of early and late onset: characterization of two types of psoriasis vulgaris., Journal of the American Academy of Dermatology, 13:450-456.

Henseler T., Christophers E. (1995). Disease concomitance in psoriasis., Journal of the American Academy of Dermatology, 32:982-986.

Hudson L.G., McCawley L.J. (1998). Contributions of the epidermal growth factor receptor to keratinocyte motility., Microscopy research and technique, 43:444-455.

Hunt T.K., Burke J., Barbul A., Gimbel M.L. (1999). Wound healing., Science, 284:1775.

Hunt TK. (1980). Wound healing and wound infection: theory and surgical practice. New York: Appleton-Century-Crofts.

Hussussian. C. J., Struewing, J. P., Goldstein, A. M., Higgins, P. A. T., Ally, D. S., Shcahan. M. D., Clark, W. H., Tucker. M. A., and Dracopoli, N. C. (1994). Germline pl6 mutations in familial melanoma., Nat. Genet, 8: 15-21

Imamura, J., Miyoshi, I., & Koeffler, H. (1994). p53 in hematologic malignancies., Blood, 84(8): 2412-2421.

Ishida, N., Hara, T., Kamura, T., Yoshida, M., Nakayama, K., & Nakayama, K. I. (2002). Phosphorylation of p27 Kip1 on serine 10 is required for its binding to CRM1 and nuclear export., Journal of Biological Chemistry, 277(17): 14355-14358.

Ito, M., Liu, Y., Yang, Z., Nguyen, J., Liang, F., Morris, R. J., & Cotsarelis, G. (2005). Stem cells in the hair follicle bulge contribute to wound repair but not to homeostasis of the epidermis., Nature medicin, 11(12): 1351-1354.

Jaks, V., Kasper, M., & Toftgรกrd, R. (2010). The hair follicleโ€“a stem cell zoo., Experimental cell research, 316(8): 1422-1428.

Jen J., Harper J.W., Bigner S.H., Bigner D.D., Papadopoulos N., Markowitz S., Willson J.K., Kinzler K.W., Vogelstein B. (1994). Deletion of p16 and p15 genes in brain tumors., Cancer Research, 54:6353-6358.

Jen, J., Harper, J. W., Bigner, S. H., Bigner, D. D., Papadopoulos, N., Markowitz, S., . . . Vogelstein, B. (1994). Deletion of p16 and p15 genes in brain tumors., Cancer Research, 54(24): 6353-6358.

Jensen K.B., Watt F.M. (2006). Single-cell expression profiling of human epidermal stem and transit-amplifying cells: Lrig1 is a regulator of stem cell quiescence., Proceedings of the National Academy of Sciences, 103:11958-11963.

Kamb, A. C. (1996). A Cell Cycle Regulator and Cancer Hormonal Carcinogenesis II (pp. 59-67): Springer.

Kamb, A., Gruis, N. A., Weaver-Feldhaus, J., Liu, Q., Harshman, K., Tavtigian, S. V., Skolnick, M. H. (1994). A cell cycle regulator potentially involved in genesis of many tumor types., Science, 264(5157): 436-440.

Kario E., Marmor M.D., Adamsky K., Citri A., Amit I., Amariglio N., Rechavi G., Yarden Y. (2005). Suppressors of cytokine signaling 4 and 5 regulate

epidermal growth factor receptor signaling., Journal of Biological Chemistry, 280:7038-7048.

Karnes W.E., Weller S.G., Adjei P.N., Kottke T.J., Glenn K.S., Gores G.J., Kaufmann S.H. (1998). Inhibition of epidermal growth factor receptor kinase induces protease-dependent apoptosis in human colon cancer cells., Gastroenterology, 114:930-939.

Kawamata N., Morosetti R., Miller C.W., Park D., Spirin K.S., Nakamaki T., Takeuchi S., Hatta Y., Simpson J., Wilczynski S. (1995). Molecular analysis of the cyclin-dependent kinase inhibitor gene p27/Kip1 in human malignancies., Cancer Research, 55:2266-2269.

Kawamata, N., Morosetti, R., Miller, C. W., Park, D., Spirin, K. S., Nakamaki, T., Wilczynski, S. (1995). Molecular analysis of the cyclin-dependent kinase inhibitor gene p27/Kip1 in human malignancies., Cancer Research, 55(11): 2266-2269.

Keilhack H., Tenev T., Nyakatura E., Godovac-Zimmermann J., Nielsen L., Seedorf K., B?hmer F.-D. (1998). Phosphotyrosine 1173 mediates binding of the protein-tyrosine phosphatase SHP-1 to the epidermal growth factor receptor and attenuation of receptor signaling., Journal of Biological Chemistry, 273:24839-24846.

Kelley, L. A., & Sternberg, M. J. (2009). Protein structure prediction on the Web: a case study using the Phyre server., Nature protocols, 4(3): 363-371.

Kessel, A., & Ben-Tal, N. (2012). Introduction to proteins: structure, function, and motion., CRC Press Letter Science, 284(5421):1775.

Kozak, M. (1997). Recognition of AUG and alternative initiator codons is augmented by G in position+ 4 but is not generally affected by the nucleotides in positions+ 5 and+ 6., The EMBO journal, 16(9): 2482-2492.

Kulik G., Klippel A., Weber M.J. (1997). Antiapoptotic signalling by the insulin-like growth factor I receptor, phosphatidylinositol 3-kinase, and Akt., Molecular and cellular biology, 17:1595-1606.

Laederich M.B., Funes-Duran M., Yen L., Ingalla E., Wu X., Carraway K.L., Sweeney C. (2004). The leucine-rich repeat protein LRIG1 is a negative regulator of ErbB family receptor tyrosine kinases., Journal of Biological Chemistry, 279:47050-47056.

Langton, A. K., Herrick, S. E., & Headon, D. J. (2007). An extended epidermal response heals cutaneous wounds in the absence of a hair follicle stem cell contribution., Journal of Investigative Dermatology, 128(5): 1311-1318.

Larjava, H., Salo, T., Haapasalmi, K., Kramer, R., & Heino, J. (1993). Expression of integrins and basement membrane components by wound keratinocytes., Journal of Clinical Investigation, 92(3): 1425.

Laskowski, R. A., MacArthur, M. W., Moss, D. S., & Thornton, J. M. (1993). PROCHECK: a program to check the stereochemical quality of protein structures., Journal of applied crystallography, 26(2): 283-291.

Lee, M.-H., Reynisdottir, I., & Massague, J. (1995). Cloning of p57KIP2, a cyclin-dependent kinase inhibitor with unique domain structure and tissue distribution., Genes & development, 9(6): 639-649.

Li, L., Li, C., Sarkar, S., Zhang, J., Witham, S., Zhang, Z., Alexov, E. (2012). DelPhi: a comprehensive suite for DelPhi software and associated resources., BMC biophysics, 5(1): 9.

Luo Y., Hurwitz J., Massagцц J. (1995). Cell-cycle inhibition by independent CDK and PCNA binding domains in p21Cip1., Nature, 375(6527): 159-61.

M Yates V., Watkinson G., Kelman A. (1982). Further evidence for an association between psoriasis, Crohn's disease and ulcerative colitis., British Journal of Dermatology, 106:323-330.

Maitra A., Wistuba I.I., Washington C., Virmani A.K., Ashfaq R., Milchgrub S., Gazdar A.F., Minna J.D. (2001). High-resolution chromosome 3p allelotyping of breast carcinomas and precursor lesions demonstrates frequent loss of heterozygosity and a discontinuous pattern of allele loss., The American journal of pathology, 159:119-130.

Mao F., Wang B., Xi G., Sun W., Zhang H., Ye F., Guo D., Lei T. (2012) Effects of RNAi-mediated gene silencing of LRIG1 on proliferation and invasion of glioma cells., Journal of Huazhong University of Science and Technology Medical Sciences, 32:227-232.

Martin, P. (1997). Wound healing--aiming for perfect skin regeneration., Science, 276(5309): 75-81.

Mascia F., Mariani V., Girolomoni G., Pastore S. (2003). Blockade of the EGF receptor induces a deranged chemokine expression in keratinocytes leading to enhanced skin inflammation., The American journal of pathology, 163:303-312.

Matsuoka S., Edwards M.C., Bai C., Parker S., Zhang P., Baldini A., Harper J.W., Elledge S.J. (1995). p57KIP2, a structurally distinct member of the p21CIP1 Cdk inhibitor family, is a candidate tumor suppressor gene., Genes & development, 9:650-662.

Matsuoka, S., Edwards, M. C., Bai, C., Parker, S., Zhang, P., Baldini, A., Elledge, S. J. (1995). p57KIP2, a structurally distinct member of the p21CIP1 Cdk inhibitor family, is a candidate tumor suppressor gene., Genes & development, 9(6): 650-662.

Mendelsohn, A. R., & Brent, R. (1999). Protein interaction methods-toward an endgame., Science, 284(5422): 1948-1950.

Moerschell, R., Hosokawa, Y., Tsunasawa, S., & Sherman, F. (1990). The specificities of yeast methionine aminopeptidase and acetylation of amino-terminal methionine in vivo. Processing of altered iso-1-cytochromes c created by oligonucleotide transformation., Journal of Biological Chemistry, 265(32): 19638-19643.

Mori, M., Mimori, K., Shiraishi, T., Tanaka, S., Ueo, H., Sugimachi, K., & Akiyoshi, T. (1997). p27 expression and gastric carcinoma., Nature medicine, 3(6): 593-593.

Morosetti R., Kawamata N., Gombart A.F., Miller C.W., Hatta Y., Hirama T., Said J.W., Tomonaga M., Koeffler H.P. (1995). Alterations of the p27KIP1 gene in non-Hodgkin's lymphomas and adult T-cell leukemia/lymphoma., Blood, 86:1924-1930.

Morosetti, R., Kawamata, N., Gombart, A. F., Miller, C. W., Hatta, Y., Hirama, T., Koeffler, H. P. (1995). Alterations of the p27KIP1 gene in non-Hodgkin's lymphomas and adult T-cell leukemia/lymphoma., Blood, 86(5): 1924-1930.

Motti M.L., De Marco C., Califano D., Fusco A., Viglietto G. (2004). Akt-dependent T198 phosphorylation of cyclin-dependent kinase inhibitor p27kip1 in breast cancer., Cell Cycle, 3:1072-1078.

Motti, M. L., De Marco, C., Califano, D., Fusco, A., & Viglietto, G. (2004). Akt-dependent T198 phosphorylation of cyclin-dependent kinase inhibitor p27kip1 in breast cancer., Cell Cycle, 3(8): 1072-1078.

Moyer J.D., Barbacci E.G., Iwata K.K., Arnold L., Boman B., Cunningham A., DiOrio C., Doty J., Morin M.J., Moyer M.P. (1997). Induction of apoptosis and cell cycle arrest by CP-358,774, an inhibitor of epidermal growth factor receptor tyrosine kinase., Cancer research, 57:4838-4848.

Muller R.A., Morris D.E. (1989). Geomagnetic reversals driven by sudden climate changes., Eos, 70:276.

Nakanishi M., Robetorye R., Adami G., Pereira-Smith O., Smith J. (1995). Identification of the active region of the DNA synthesis inhibitory gene p21Sdi1/CIP1/WAF1., The EMBO journal, 14:555.

Nakanishi, M., Robetorye, R., Adami, G., Pereira-Smith, O., & Smith, J. (1995). Identification of the active region of the DNA synthesis inhibitory gene p21Sdi1/CIP1/WAF1., The EMBO journal, 14(3): 555.

Nanney L.B., Mckanna J.A., Stoscheck C.M., Carpenter G., King L.E. (1984). Visualization of epidermal growth factor receptors in human epidermis., Journal of Investigative Dermatology, 82:165-169.

Nanney, L. B., Paulsen, S., Davidson, M. K., Cardwell, N. L., Whitsitt, J. S., & Davidson, J. M. (2000). Boosting epidermal growth factor receptor expression by gene gun transfection stimulates epidermal growth in vivo., Wound Repair and Regeneration, 8(2): 117-127.

Nicholson S.E., Metcalf D., Sprigg N.S., Columbus R., Walker F., Silva A., Cary D., Willson T.A., Zhang J.-G., Hilton D.J. (2005). Suppressor of cytokine signaling (SOCS)-5 is a potential negative regulator of epidermal growth factor signaling., Proceedings of the National Academy of Sciences of the United States of America, 102:2328-2333.

Nobori, T. (1994). Deletions of the cyclin-dependent kinase-4 inhibitor gene in multiple human cancers., Trends in Genetics, 10(7): 228.

Nyati M.K., Morgan M.A., Feng F.Y., Lawrence T.S. (2006). Integration of EGFR inhibitors with radiochemotherapy., Nature Reviews Cancer, 6:876-885.

Ogiso H., Ishitani R., Nureki O., Fukai S., Yamanaka M., Kim J.-H., Saito K., Sakamoto A., Inoue M., Shirouzu M. (2002). Crystal structure of the complex

of human epidermal growth factor and receptor extracellular domains., Cell, 110:775-787.

Olayioye M.A., Neve R.M., Lane H.A., Hynes N.E. (2000). The ErbB signaling network: receptor heterodimerization in development and cancer., The EMBO journal, 19:3159-3167.

Opalenik S.R., Davidson J.M. (2005). Fibroblast differentiation of bone marrow-derived cells during wound repair., The FASEB Journal, 19:1561-1563.

Owens D.M., Watt F.M. (2003). Contribution of stem cells and differentiated cells to epidermal tumours., Nature Reviews Cancer, 3:444-451.

Panelos J., Massi D. (2009). Emerging role of Notch signaling in epidermal differentiation and skin cancer., Cancer Biol Ther, 8:1986-1993.

Pastore S., Mascia F., Mariani V., Girolomoni G. (2007). The epidermal growth factor receptor system in skin repair and inflammation., Journal of Investigative Dermatology, 128:1365-1374.

Polyak K., Lee M.-H., Erdjument-Bromage H., Koff A., Roberts J.M., Tempst P., Massague J. (1994) Cloning of p27< sup> Kip1</sup>, a cyclin-dependent kinase inhibitor and a potential mediator of extracellular antimitogenic signals., Cell, 78:59-66.

Polyak, K., Lee, M.-H., Erdjument-Bromage, H., Koff, A., Roberts, J. M., Tempst, P., & Massague, J. (1994). Cloning of p27< sup> Kip1</sup>, a cyclin-dependent kinase inhibitor and a potential mediator of extracellular antimitogenic signals., Cell, 78(1): 59-66.

Ponce-Castaร ฑeda M.V., Lee M.-H., Latres E., Polyak K., Lacombe L., Montgomery K., Mathew S., Krauter K., Sheinfeld J., Massague J. (1995). p27Kip1: chromosomal mapping to 12p12-12p13. 1 and absence of mutations in human tumors., Cancer Research, 55:1211-1214.

Powell A.E., Wang Y., Li Y., Poulin E.J., Means A.L., Washington M.K., Higginbotham J.N., Juchheim A., Prasad N., Levy S.E. (2012). The pan-ErbB negative regulator Lrig1 is an intestinal stem cell marker that functions as a tumor suppressor., Cell, 149:146-158.

Prakash I., Mathur R., Kar P., Ranga S., Talib V. (1997). Comparative evaluation of cell proliferative indices and epidermal growth factor receptor expression in gastric carcinoma., Indian Journal of Pathology and Microbiology, 40:481.

Radinsky R., Risin S., Fan D., Dong Z., Bielenberg D., Bucana C.D., Fidler I.J. (1995). Level and function of epidermal growth factor receptor predict the metastatic potential of human colon carcinoma cells., Clinical cancer research, 1:19-31.

Repertinger S.K., Campagnaro E., Fuhrman J., El-Abaseri T., Yuspa S.H., Hansen L.A. (2004). EGFR enhances early healing after cutaneous incisional wounding., Journal of Investigative Dermatology, 123:982-989.

Roberson E., Bowcock A.M. (2010). Psoriasis genetics: breaking the barrier., Trends in genetics, 26:415-423.

Robinson D.R., Wu Y.-M., Lin S.-F. (2000). The protein tyrosine kinase family of the human genome., Oncogene, 19:5548-5557.

Rodier G., Montagnoli A., Di Marcotullio L., Coulombe P., Draetta G.F., Pagano M., Meloche S. (2001). p27 cytoplasmic localization is regulated by phosphorylation on Ser10 and is not a prerequisite for its proteolysis., The EMBO journal, 20:6672-6682.

Rodier, G., Montagnoli, A., Di Marcotullio, L., Coulombe, P., Draetta, G. F., Pagano, M., & Meloche, S. (2001). p27 cytoplasmic localization is regulated by phosphorylation on Ser10 and is not a prerequisite for its proteolysis., The EMBO journal, 20(23): 6672-6682.

Roussel M.F. (1999). The INK4 family of cell cycle inhibitors in cancer., Oncogene, 18:5311-5317.

Roussel, M. F. (1999). The INK4 family of cell cycle inhibitors in cancer., Oncogene, 18(38): 5311-5317.

Ruiz D.G., Azevedo M.N.L.d., Santos O.L.d.R. (2012). Psoriatic arthritis: a clinical entity distinct from psoriasis? Revista brasileira de reumatologia, 52:630-638.

Russo, A. A., Jeffrey, P. D., Patten, A. K., Massagui, J., & Pavletich, N. P. (1996). Crystal structure of the p27Kip1 cyclin-dependent-kinase inhibitor bound to the cyclin A-Cdk2 complex., Nature, 382(6589): 325-331.

Salomon D.S., Brandt R., Ciardiello F., Normanno N. (1995). Epidermal growth factor-related peptides and their receptors in human malignancies., Critical reviews in oncology/hematology, 19:183-232.

Schneider M.R., Wolf E. (2008). The epidermal growth factor receptor and its ligands in female reproduction: insights from rodent models., Cytokine & growth factor reviews, 19:173-181.

Segatto O., Anastasi S., Alems S. (2011). Regulation of epidermal growth factor receptor signalling by inducible feedback inhibitors., Journal of cell science, 124:1785-1793.

Sekimoto, T., Fukumoto, M., and Yoneda, Y. (2004). 14-3-3 suppresses the nuclear localization of threonine 157-phosphorylated p27Kip1., The EMBO Journal, 23: 1934–1942.

Sgambato, A., Cittadini, A., Faraglia, B., & Weinstein, I. B. (2000). Multiple functions of p27Kip1 and its alterations in tumor cells: a review., Journal of cellular physiology, 183(1): 18-27.

Sherr, C. J., & Roberts, J. M. (1999). CDK inhibitors: positive and negative regulators of G1-phase progression., Genes & development, 13(12): 1501-1512.

Sheu J.J.-C., Lee C.-H., Ko J.-Y., Tsao G.S., Wu C.-C., Fang C.-Y., Tsai F.-J., Hua C.-H., Chen C.-L., Chen J.-Y. (2009). Chromosome 3p12. 3-p14. 2 and 3q26. 2-q26. 32 are genomic markers for prognosis of advanced nasopharyngeal carcinoma., Cancer Epidemiology Biomarkers & Prevention, 18:2709-2716.

Shin I., Yakes F.M., Rojo F., Shin N.-Y., Bakin A.V., Baselga J., Arteaga C.L. (2002). PKB/Akt mediates cell-cycle progression by phosphorylation of p27Kip1 at threonine 157 and modulation of its cellular localization., Nature medicine, 8:1145-1152.

Shin, I., Yakes, F. M., Rojo, F., Shin, N.-Y., Bakin, A. V., Baselga, J., & Arteaga, C. L. (2002). PKB/Akt mediates cell-cycle progression by phosphorylation of p27Kip1 at threonine 157 and modulation of its cellular localization., Nature medicine, 8(10): 1145-1152.

Slingerland, J., & Pagano, M. (2000). Regulation of the Cdk inhibitor p 27 and its deregulation in cancer., Journal of cellular physiology, 183(1): 10-17.

Sorkin A., Goh L.K. (2009). Endocytosis and intracellular trafficking of ErbBs., Experimental cell research, 315:683-696.

Spirin, K. S., Simpson, J. F., Takeuchi, S., Kawamata, N., Miller, C. W., & Koeffler, H. P. (1996). p27/Kip1 mutation found in breast cancer., Cancer Research, 56(10): 2400-2404.

Stadelmann, W. K., Digenis, A. G., & Tobin, G. R. (1998). Physiology and healing dynamics of chronic cutaneous wounds., The American Journal of Surgery, 176(2): 26S-38S.

Stoll, S., Garner, W., & Elder, J. (1997). Heparin-binding ligands mediate autocrine epidermal growth factor receptor activation In skin organ culture., Journal of Clinical Investigation, 100(5): 1271.

Stoscheck, C. M., Nanney, L. B., & King, L. E. (1992). Quantitative determination of EGF-R during epidermal wound healing., Journal of Investigative Dermatology, 99(5): 645-649.

Stutz M.A., Shattuck D., Laederich M., Carraway K., Sweeney C. (2008). LRIG1 negatively regulates the oncogenic EGF receptor mutant EGFRvIII., Oncogene, 27:5741-5752.

Suzuki, Y., Miura, H., Tanemura, A., Kobayashi, K., Kondoh, G., Sano, S., Itami, S. (2002). Targeted disruption of LIG-1 gene results in psoriasiform epidermal hyperplasia. [Research Support, Non-U.S. Gov't]. FEBS letters, 521(1-3): 67-71.

Susan F. Steinberg. (2008). Structural Basis of Protein Kinase C Isoform Function., Physiological Reviews, 1 **(**88): 1341-1378

Tanemura A, Nagasawa T, Inui S, Itami S (2005). LRIG-1 provides a novel prognostic predictor in squamous cell carcinoma of the skin: immunohistochemical analysis for 38 cases., Dermatol Surg, 31: 423-30

Tomic-Canic M., Komine M., Freedberg I.M., Blumenberg M. (1998). Epidermal signal transduction and transcription factor activation in activated keratinocytes., Journal of dermatological science, 17:167-181.

Tomoda, K., Kubota, Y., & Kato, J.-y. (1999). Degradation of the cyclin-dependent-kinase inhibitor p27Kip1 is instigated by Jab1., Nature, 398(6723), 160-165.

Toyoshima, H., & Hunter, T. (1994). p27, a novel inhibitor of G1 cyclin-Cdk protein kinase activity, is related to p21. Cell; 78(1): 67-74.

Turkeri, L. N., Erton, M. L., Cevik, I. and Akdas, A.(1998). Impact of the expression of epidermal growth factor, transforming growth factor alpha, and epidermal

growth factor receptor on the prognosis of superficial bladder cancer., Urology, 51: 645–649

Viglietto G., Motti M.L., Bruni P., Melillo R.M., D'alessio A., Califano D., Vinci F., Chiappetta G., Tsichlis P., Bellacosa A. (2002). Cytoplasmic relocalization and inhibition of the cyclin-dependent kinase inhibitor p27Kip1 by PKB/Akt-mediated phosphorylation in breast cancer., Nature medicine, 8(10):1136-1144.

Wade Harper, J., Adami, G. R., Wei, N., Keyomarsi, K., & Elledge, S. J. (1993). The p21 Cdk-interacting protein Cip1 is a potent inhibitor of G1 cyclin-dependent kinases., Cell, 75(4): 805-816.

Wang B., Han L., Chen R., Cai M., Han F., Lei T., Guo D.-S. (2009). Down-regulation of LRIG2 expression by RNA interference inhibits glioblastoma cell (GL15) growth, causes cell cycle redistribution, increases cell apoptosis and enhances cell adhesion and invasion in vitro., Cancer biology & therapy, 8:1018-1023.

Wang Y., Poulin E., Coffey R. (2013). LRIG1 is a triple threat: ERBB negative regulator, intestinal stem cell marker and tumour suppressor., British journal of cancer, 108:1765-1770.

Wang, X., Ge, J., Tredget, E. E., & Wu, Y. (2013). The mouse excisional wound splinting model, including applications for stem cell transplantation., Nature protocols, 8(2): 302-309.

Wenczak, B. A., Lynch, J. B., & Nanney, L. B. (1992). Epidermal growth factor receptor distribution in burn wounds. Implications for growth factor-mediated repair., Journal of Clinical Investigation, 90(6): 2392.

Werner S., Grose R. (2003). Regulation of wound healing by growth factors and cytokines., Physiological reviews, 83:835-870.

Werner S., Krieg T., Smola H. (2007). Keratinocyte and fibroblast interactions in wound healing., Journal of Investigative Dermatology, 127:998-1008.

Wong, V. W., Stange, D. E., Page, M. E., Buczacki, S., Wabik, A., Itami, S., van de Wetering M., Poulsom R., Wright N.A., Trotter, M. W. (2012). Lrig1 controls intestinal stem-cell homeostasis by negative regulation of ErbB signalling., Nature cell biology, 14(4): 401-408.

Wu, W.I., Voegtli, W. C., Sturgis, H. L., Dizon, F. P., Vigers, G. P., & Brandhuber, B. J. (2010). Crystal structure of human AKT1 with an allosteric inhibitor reveals a new mode of kinase inhibition., PLoS One, 5(9): e12913.

Yarden Y. (2001). The EGFR family and its ligands in human cancer: signalling mechanisms and therapeutic opportunities., European Journal of Cancer, 37:3-8.

Willers CP, Siebert R, BardenheuerW, Lux A,Michaelis S, Seeber S, Luboldt HJ, Opalka B, Schutte J. (1996). Genetic instability of 3p12-p21-specific microsatellite sequences in renal cell carcinoma., Br J Urol, 77:524–529.